Published in final edited form as:

Arterioscler Thromb Vasc Biol. 2023 August ; 43(8): e303–e322. doi:10.1161/ATVBAHA.122.318173.

Endothelial PHACTR1 promotes endothelial activation and atherosclerosis by repressing PPARγ activity under disturbed flow in mice

Dongyang Jiang[1,*,†], **Hao Liu**[1,*], **Guofu Zhu**[1,*], **Xiankai Li**[1], **Linlin Fan**[1], **Faxue Zhao**[1], **Chong Xu**[1], **Shumin Wang**[2], **Yara Rose**[2], **Jordan Rhen**[2], **Ze Yu**[1], **Yiheng Yin**[1], **Yuling Gu**[3], **Xiangbin Xu**[2], **Edward A. Fisher**[4], **Junbo Ge**[1], **Yawei Xu**[1,†], **Jinjiang Pang**[2,†]

[1]Department of Cardiology, Pan-vascular Research Institute, Shanghai Tenth People's Hospital, Tongji University School of Medicine, Shanghai 200072, China (D. J., H. L., G. Z., X. L., L. F., F. Z., C. X., Z. Y., Y. Y., J. G., Y. X.)

[2]Aab Cardiovascular Research Institute, Department of Medicine and Dentistry, University of Rochester, Rochester, NY 14642, USA (S. W., Y. R., J. R., X. X., J. P.)

[3]Shanghai Naturethink Life Science&Technology Co., ltd, Shanghai 201809, China (Y. G.)

[4]Division of Cardiology, Department of Medicine, New York University School of Medicine, New York, NY 10016, USA (E. A. F.)

Abstract

BACKGROUND: Numerous genome-wide association studies revealed that SNPs at phosphatase and actin regulator 1 (*PHACTR1*) locus strongly correlate with coronary artery disease (CAD). However, the biological function of PHACTR1 remains poorly understood. Here, we identified the pro-atherosclerotic effect of endothelial PHACTR1, contrary to macrophage PHACTR1.

METHODS: We generated global (*Phactr1*$^{-/-}$) and endothelial cell (EC)-specific (*Phactr1*^{ECKO}) *Phactr1* knockout mice and crossed these mice with apolipoprotein E-deficient (*Apoe*$^{-/-}$) mice. Atherosclerosis was induced by feeding the high-fat/high-cholesterol (HF-HC) diet for 12 weeks or partially ligating carotid arteries combined with a 2-week HF-HC diet. PHACTR1 localization was identified by immunostaining of overexpressed PHACTR1 in human umbilical vein endothelial cells (HUVECs) exposed to different types of flow. The molecular function of endothelial PHACTR1 was explored by RNA sequencing using EC-enriched mRNA from

[†]Corresponding authors: Jinjiang Pang, Aab Cardiovascular Research Institute, Department of Medicine and Dentistry, University of Rochester, Rochester, NY 14642, USA. Phone: 585-276-7707; jinjiang_pang@urmc.rochester.edu.; Dongyang Jiang, Department of Cardiology, Pan-vascular Research Institute, Shanghai Tenth People's Hospital, Tongji University School of Medicine, Shanghai 200072, China. Phone: 86-21-66302089; jiangdy@tongji.edu.cn.; Yawei Xu, Department of Cardiology, Pan-vascular Research Institute, Shanghai Tenth People's Hospital, Tongji University School of Medicine, Shanghai 200072, China. Phone: 86-21-66302089, xuyawei@tongji.edu.cn.

[*]Dongyang Jiang, Hao Liu and Guofu Zhu contributed equally.

Disclosures

None.

Supplemental Material

Expanded materials and methods

Figures S1–S6

Tables S1–S10

global or EC-specific *Phactr1* knockout mice. Endothelial activation was evaluated in HUVECs transfected with siRNA targeting *PHACTR1* and in *Phactr1*^{ECKO} mice after partial carotid ligation.

RESULTS: Global or EC-specific *Phactr1* deficiency significantly inhibited atherosclerosis in regions of disturbed flow. PHACTR1 was enriched in ECs and located in the nucleus of disturbed flow areas but shuttled to cytoplasm under laminar flow *in vitro*. RNA sequencing showed that endothelial *Phactr1* depletion affected vascular function and peroxisome proliferator-activated receptor gamma (PPARγ) was the top transcription factor regulating differentially expressed genes. PHACTR1 functioned as a PPARγ transcriptional corepressor by binding to PPARγ through the corepressor motifs. PPARγ activation protects against atherosclerosis by inhibiting endothelial activation. Consistently, *PHACTR1* deficiency remarkably reduced endothelial activation induced by disturbed flow *in vivo* and *in vitro*. PPARγ antagonist GW9662 abolished the protective effects of *Phactr1* knockout on EC activation and atherosclerosis *in vivo*.

CONCLUSIONS: Our results identified endothelial PHACTR1 as a novel PPARγ corepressor to promote atherosclerosis in disturbed flow regions. Endothelial PHACTR1 is a potential therapeutic target for atherosclerosis treatment.

Graphical Abstract

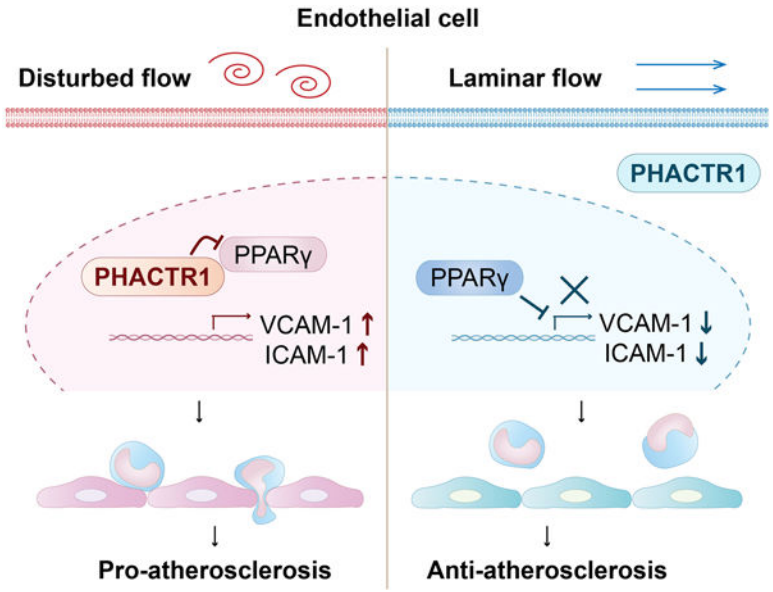

Keywords

PHACTR1; atherosclerosis; endothelial activation; PPARγ; shear stress

INTRODUCTION

Coronary artery disease (CAD) caused by atherosclerosis is the leading cause of death worldwide. Blood clots formed after the rupture of atherosclerotic plaques can cause complete blockage of the coronary artery, leading to myocardial infarction and even death.[1] Atherosclerotic plaques preferentially form in the disturbed flow region, such as arterial

bifurcations, where disturbed flow causes endothelial activation.[2, 3] Activated endothelial cells (ECs) increase expression of adhesion molecules such as vascular cell adhesion molecule 1 (VCAM-1), intercellular cell adhesion molecule 1 (ICAM-1), and E-selectin, which facilitate leukocyte attachment on endothelial surfaces and migration into the intima.[4] Although extensive studies have revealed that endothelial activation induced by irritative stimuli is an important early step of atherosclerosis, the underlying mechanisms remain elusive.

Phosphatase and actin regulator 1 (PHACTR1), belonging to a highly conserved PHACTR family, was first discovered as a PP1 (protein phosphatase 1)-binding protein in the brain in 2004.[5] In the last decade, several large-scale genome-wide association studies (GWAS) from different cohorts and different research groups showed that SNPs at the *PHACTR1* locus are significantly associated with the onset, progression, and outcome of CAD and myocardial infarction in humans.[6–11] According to the Genotype-Tissue Expression (GTEx) database[12] and prior biological studies, these SNPs are expression quantitative trait loci (eQTL) of *PHACTR1*, that is, they are correlated with *PHACTR1* mRNA expression,[13–15] suggesting that PHACTR1 is the causal gene. Recently Kasikara *et al* reported that *Phactr1*-deficient bone marrow aggravated atherosclerosis *in vivo*.[14] The mechanistic studies revealed that macrophage PHACTR1 was involved in efferocytosis and macrophage differentiation to inhibit atherosclerosis.[13, 14]

Intriguingly, our analysis of the GTEx database revealed that CAD-related PHACTR1 SNPs were associated with PHACTR1 mRNA expression and that the associations are mainly in non-diseased arteries but not in the nervous system, immune system, or other tissue, highlighting the potential role of PHACTR1 derived from non-immune vascular cells in atherosclerosis. In human vessels, PHACTR1 is also enriched in ECs.[16] However, the functions of endothelial PHACTR1 were only explored *in vitro* using siRNA, and the conclusions were controversial: Jarray *et al* demonstrated that endothelial PHACTR1 was protective by decreasing the expression of thrombin, thrombin receptor 1, and so on in human umbilical vein endothelial cells (HUVECs) under basal conditions,[17] while Zhang *et al* proved that PHACTR1 was athero-prone through inducing VCAM-1 and ICAM-1 expression in human coronary artery endothelial cells after ox-LDL stimulation.[18] The inconsistency is possible due to different cell types and different experimental conditions in these *in vitro* experiments. Although GWAS demonstrated the association of *PHACTR1* locus with hypertension, recent *in vivo* studies indicated that global or SMC- or EC-specific *Phactr1* deletion did not affect blood pressure and vascular response to hypertension.[19, 20] Therefore, it is essential to define whether endothelial PHACTR1 was involved in atherosclerosis using EC-specific *Phactr1*-deficient mice *in vivo*. Moreover, global *Phactr1* knockout mice should be analyzed thoroughly to evaluate the synergistic roles of endothelial PHACTR1 and macrophage PHACTR1 in atherosclerosis. Notwithstanding, Li *et al* generated $Phactr1^{-/-}$ mice by targeting exon 2–3, and these knockout mice had increased atherosclerosis lesions.[13] Unfortunately, targeting this exon was unable to knock down the major isoform of vascular *PHACTR1*, which lacks exon 2–3.

In the current study, we defined the role of *Phactr1* in atherosclerosis *in vivo* using global and EC-specific *Phactr1* knockout mice. These mice were generated by targeting exon 7, and

Phactr1 depletion was confirmed. PHACTR1 expression was enriched in murine ECs. Loss of global or endothelial *Phactr1* in apolipoprotein E knockout ($Apoe^{-/-}$) mice significantly attenuated the high-fat, high-cholesterol (HF-HC) diet-induced atherosclerosis, specifically in disturbed flow regions. Mechanistic studies revealed that endothelial PHACTR1 was located in the nucleus under disturbed flow to promote EC activation through repressing peroxisome proliferator-activated receptor gamma (PPARγ) transcriptional activity.

MATERIALS AND METHODS

Data access

The data supporting this study's findings are available from the corresponding author upon reasonable request.

Mice

Phactr1 global knockout ($Phactr1^{-/-}$) and floxed ($Phactr1^{f/f}$) mice in C57BL/6J background were generated through CRISPR/Cas9 system targeting exon 7 of *Phactr1* (ENSMUST00000128646) by Beijing Biocytogen Co., Ltd. The sequences of small guide RNAs (sgRNAs) were 5'-GCCCAGGTAGGATGGCATCAGG-3' (sgRNA1) and 5'-GTATGTACTGTCATGTCTGG-3' (sgRNA2) (PAM sequences were underlined). $Apoe^{-/-}$ mice (B6.129P2-$Apoe^{tm1Unc}$/J) and *Tie2*-Cre mice (B6.Cg-Tg(Tek-cre)1Ywa/J) were purchased from Jackson Laboratory. Endothelial-specific *Phactr1* knockout ($Phactr1^{ECKO}$) mice were generated by crossbreeding $Phactr1^{f/f}$ mice with *Tie2*-Cre mice. $Phactr1^{-/-}$ mice and $Phactr1^{ECKO}$ mice were further mated with $Apoe^{-/-}$ mice to generate $Phactr1^{-/-}Apoe^{-/-}$ and $Phactr1^{ECKO}Apoe^{-/-}$ mice. Only male mice were used in this study, since the associations of *PHACTR1* with CADs were mainly identified in elderly men and women (postmenopausal). All mice were housed in a specific pathogen-free facility at Tongji University, under a 12 h light/dark cycle (light from 7 AM to 7 PM local time), and had *ad libitum* access to food and water. All animal procedures were approved by the Animal Care and Use Committees of Shanghai Tenth People's Hospital (SHDSYY-0050, SHDSYY-2020-T0009). The experiments outlined in this manuscript conform to the Guide for the Care and Use of Laboratory Animals published by the National Institutes of Health (NIH Publication, 8th Edition, 2011).

Cell culture

HUVECs from different donors were purchased from ScienCell (ScienCell Research Laboratories). HUVEC were cultured in endothelial culture medium (ScienCell Research Laboratories) supplemented with 5% fetal bovine serum (FBS, Gibco), 1% endothelial cell growth supplement (ScienCell Research Laboratories), 1% penicillin-streptomycin at 37°C in 95% CO_2. Passages 3 to 6 were used for experiments. 293FT cells were maintained in Dulbecco's Modified Eagle Medium (Thermo Fisher Scientific) supplemented with 10% FBS, and 1% penicillin-streptomycin at 37°C in 95% CO_2. Peripheral blood mononuclear cells (PBMCs) were isolated from peripheral blood of healthy donors (64 years old, male) using Ficoll/Hypaque (Sigma-Aldrich) density-gradient centrifugation as previously described.[21] PBMCs at the interface were recovered and washed with PBS, and the isolated PBMCs were used for further experiments. Written informed consents were obtained from

all donors. All procedures were performed with the ethical approval of the Clinical Research Ethics Committee of the Shanghai Tenth People's Hospital.

HF-HC diet-induced atherosclerosis model

The atherosclerotic model was performed and analyzed following the guidelines for experimental atherosclerosis studies described in the AHA Statement.[22] 8-week-old male mice (littermates) were fed a HF-HC diet supplemented with 21% (w/w) fat, 1.3% (w/w) cholesterol, and 0.3% (w/w) cholate (Shanghai Laboratory Animal Center, SLAC, Chinese Academy of Sciences) to develop atherosclerosis. After 12 weeks, mice were euthanized by an overdose of pentobarbital (150 mg/kg, i.p.) and atherosclerotic lesions were characterized as described previously.[22, 23]

En face staining of mouse aortas

After euthanasia, mice were perfused with saline containing 10 U/ml heparin via the left ventricle. For *en face* atherosclerosis analysis, aortas were prepared from the aortic arch until 3–5 mm after the aortic-common iliac bifurcation and fixed in 10% neutral buffered formalin overnight. Subsequently, peri-adventitial tissues were gently removed. Vessels were cut longitudinally to expose the intimal surface, stained with freshly-prepared oil red O solution (Sigma-Aldrich), and mounted in the glycerin gelatin mounting medium (Servicebio). Lesion areas were traced manually, measured using ImageJ software and quantified relative to the total surface area by 2 individuals in a blind manner as follows: % lesion area = (atherosclerotic lesion area/intimal area of the aorta) x 100%. Lesions from aortic arches and thoracic/abdominal aortas were quantified respectively.

For *en face* immunostaining, aortic arches were isolated and cut longitudinally to expose the endothelium, followed by 4% PFA fixation for 30 minutes on ice. After PBS washing 3 times, vessels were permeabilized with 0.3% Triton X-100 in PBS for 10 minutes, incubated with primary antibodies against VCAM-1 (Cell Signaling Technology), VE-cadherin (BD Bioscience) overnight at 4°C and fluorescein-conjugated corresponding secondary antibodies (Yeasen Biotechnology) for one hour at room temperature. Nuclei were stained with Hoechst33342. Images were obtained using Zeiss LSM710 laser confocal microscope (Zeiss) and quantified using ImageJ software blindly.

Histochemical analysis of atherosclerotic lesions in aortic roots

Heart tissues containing the aortic root were fixed in 10% neutral buffered formalin overnight, and embedded in OCT compounds (Sakura Finetek). 8-μm frozen serial sections were prepared through the aortic sinus and 40–50 sections per mouse were obtained from the origin of aortic valves. Three to four sections at about 100-μm intervals per sample were analyzed by Masson's trichrome staining or oil red O staining to evaluate lesions throughout the aortic sinus. Images were captured using the Olympus IX83 fluorescence microscope (Olympus). Lesion areas were determined blindly by ImageJ software and the mean values of three to four sections were used as the summary parameter.

Partial carotid ligation model

Partial carotid ligation was performed in 8-week-old male mice (littermates) to trigger disturbed flow-induced atherosclerosis as previously described.[24] Mice were anesthetized with continuous 2% isoflurane inhalation. Three out of four branches of the left carotid artery (LCA), including the external carotid artery, internal carotid artery and occipital artery, were ligated with a 6–0 silk suture, and the other branch (superior thyroid artery) was left open. After surgery, mice were fed the HF-HC diet for two weeks to develop atherosclerosis in LCA. For GW9662 treatment, mice received once daily treatment of GW9662 (Sigma-Aldrich, 1mg/kg body weight, i.p.) from pre-surgery day 2 to post-surgery day 14.

On post-surgery day 14, Mice were euthanized by an overdose of pentobarbital (150 mg/kg, i.p.) and perfused with cold PBS containing 10 U/mL heparin. Carotid arteries were harvested and 8-μm frozen sections were prepared as described before.[24] Cross sections of the entire carotid arteries were prepared with about 10 segments located at 200-μm intervals from the carotid bifurcation. One section from each segment was selected for analysis. Atherosclerotic lesions in each section were evaluated by oil red O staining. Infiltrated macrophages were stained with anti-CD68 antibody (Servicebio) followed by HRP-conjugated anti-rabbit secondary antibody, and amplified by VECTASTAIN® ABC Kits (Vector Laboratories). Images were captured using an Olympus IX83 fluorescence microscope (Olympus). Lesion areas and macrophages were quantified blindly using ImageJ software and the mean values of ten sections was used as the summary parameter of each vessel.

For the partial ligation-induced endothelial activation model, we used 8-week-old *Phactr1*^{ECKO} and *Phactr1*$^{f/f}$ control mice. Three days after surgery, intimal RNA was collected from the LCA and the right carotid artery (RCA) for further analysis. For GW9662 treatment, *Phactr1*^{ECKO} and *Phactr1*$^{f/f}$ mice received 5 days of once daily treatment of GW9662 (Sigma-Aldrich, 1mg/kg body weight, i.p.) from pre-surgery day 2 to post-surgery day 2.

Polymerase Chain Reaction (PCR) and western blot

Mice tissues were ground to powder in liquid nitrogen. Total RNA was extracted from HUVECs or tissue powders using Trizol reagent (Thermo Fisher Scientific). Reverse transcription was performed using 1 μg of RNA with a PrimeScript RT reagent Kit (Takara). mRNA expression was determined by PCR using TaKaRa Taq™ assay (Takara). The relative mRNA expression levels were determined by real-time PCR using SYBR Premix Ex Taq assay (Takara) and calculated using the 2-ΔΔCt method normalized to the housekeeping gene GAPDH. Primer sequences used in PCR are documented in Table S10.

For western blot, HUVECs, 293FT cells or ground mice tissues were lysed in ice-cold cell lysis buffer (Cell Signaling Technologies) containing protease inhibitor cocktail (Sigma-Aldrich). Protein concentrations were determined by BCA protein assay. 10 μg cell extracts or 10–50 μg tissue extracts were separated on SDS-PAGE and transferred to nitrocellulose membranes. After blocking with 5% milk in TBST, the membranes were incubated with the

primary antibodies against PHACTR1 (Genetex), VCAM-1 (Cell Signaling Technology), ICAM-1 (Santa Cruz Biotechnology), HA-tag (Cell Signaling Technology), Myc-tag (Cell Signaling Technology), FLAG-tag (Cell Signaling Technology), GAPDH (Millipore), and HRP-conjugated secondary antibodies, followed by ECL Western Blotting Substrate (Tanon). Images were visualized using Amersham Imager 600 system (GE Healthcare).

Mouse aortic endothelial protein extraction

Mouse aortic EC protein was extracted as described previously.[25] Briefly, mice were euthanatized by CO_2 inhalation and perfused from the left ventricle with cold saline containing 10 U/mL heparin. The aortic arch and thoracic aorta were isolated and peri-adventitial tissues were removed carefully. Then vessels were cut longitudinally and laid on the parafilm with the intima side up. 20 μL lysis buffer was dropped on the intima for 10 minutes and then collected. Other tissues were washed with PBS and incubated in digestion solutions containing 175 U/mL collagenase II (Worthington) and 1.25 U/mL elastase (Sigma-Aldrich) for 30 minutes. The media and adventitia were separated and used for further experiments.

Adenovirus infection

PHACTR1 isoform D-overexpressing adenovirus (adeno-HA-PHACTR1-D, with HA tag) was generated by GeneChem Technologies using AdMax recombinant adenovirus packaging system. HUVECs were seeded on a coverslip and reached 40–50% confluence the next day. Then adeno-HA-PHACTR1-D was added into HUVECs at an MOI of 100. 48 hours later, transfected cells were grown to confluence and put in the flow chamber for further flow treatment.

Flow experiments *in vitro*

Flow experiments were conducted using the commercial parallel-plate flow chamber (Naturethink company), which is established by sandwiching a silicon gasket between two stainless-steel plates. The chamber was perfused with complete ECM from one direction to form laminar flow (LF) or connected to a commutator to form oscillatory disturbed flow (DF). The shear stress (τ) can be estimated as $6Q\mu/wh^2$, where Q is the flow rate and μ is the viscosity of medium. Adenovirus- or siRNA-transfected HUVECs were exposed to either LF (12 dynes/cm^2) or oscillatory DF (±6 dynes/cm^2, 1 Hz).

Immunofluorescence staining

Cells were fixed with 4% PFA for 20 minutes, permeabilized with 0.3% Triton X-100 in PBS for 10 minutes, and blocked in 5% goat serum in PBS for 30 minutes. Then cells were incubated overnight at 4°C with primary antibodies against HA-tag (Cell Signaling Technology), VE-cadherin (BD Bioscience), VCAM-1 (Cell Signaling Technology), and ICAM-1 (Santa Cruz Biotechnology), and fluorescein-conjugated corresponding secondary antibodies (Yeasen Biotechnology) for one hour at room temperature. Immunostaining with non-immune isotype controls of primary antibodies was performed as negative controls. Nuclei were stained with Hoechst33342. Images were obtained using Zeiss LSM710 laser confocal microscope (Zeiss).

Mouse arterial endothelial RNA isolation

EC-enriched arterial RNA was isolated from mice as previously described.[26, 27] Mice were euthanized by CO_2 inhalation and perfused with saline containing 10 U/ml heparin via the left ventricle. Aortic arches or carotid arteries were isolated separately and peri-adventitial tissues were removed carefully. A 29-gauge syringe filled with 250 μl of QIAzol lysis reagent (QIAGEN) was inserted into the artery end and quickly flushed the aorta (~1 second). Intima eluates were used for RNA isolation using the miRNeasy mini kit (QIAGEN) following the manufacturer's protocol. VE-cadherin (endothelial cell marker) and α-smooth muscle actin (α-SMA, smooth muscle cell marker) were used to determine the enrichment of endothelial RNA.

RNA sequencing (RNA-seq) and bioinformatics

RNA-seq analysis was conducted by 10K Genomics company and Shanghai OE Biotech. For *Phactr1*$^{-/-}$ and *Phactr1*$^{+/+}$ mice, RNA-seq analysis was conducted using EC-enriched aortic RNA isolated from three mice (littermates) of 10–12 weeks old per each group. Briefly, the libraries were constructed using TruSeq Stranded mRNA LTSample Prep Kit (Illumina) according to the manufacturer's instructions. Then these libraries were sequenced on the Illumina HiSeq X Ten sequencing platform and 150bp paired-end reads were generated. Raw data (raw reads) were processed using the NGS QC Toolkit for quality control and to remove reads containing adaptors and ploy-N, and low-quality reads.[28] Clean reads were obtained and mapped to reference genome GRCm38 using the Hisat2 software version 2.0.5.[29] Fragments Per Kilobase of exon model per Million mapped fragments (FPKM) value of each gene was calculated using the Cufflinks software version 2.1.1[30] and the read counts of each gene were obtained by the HTSeq-count software version 0.6.0.[31] Differentially expressed genes (DEGs) were identified using the DESeq software 2012 (R package version 3.1.1).[32] P value < 0.05 and fold change >2 or fold change < 0.5 was set as the threshold for significantly differential expression.

For *Phactr1*^{ECKO}*Apoe*$^{-/-}$ and *Phactr1*$^{f/f}$*Apoe*$^{-/-}$ mice, four pairs of 8-week-old littermates were used. Smart-seq2 was performed using EC-enriched aortic RNA as previously described.[33] After reverse transcription and cDNA amplification, cDNA was purified using the AMPure XP beads and the library was made using the Illumina Nextera kit with indexed S5 and N7 primers according to the manufacturer's instructions. Then the library was size selected between 200–700 bp using the AMPure XP beads, and was examined using qPCR. These libraries were sequenced on the Novaseq 6000 sequencing platform and the read length was 150 bp with a pair-end strategy. Raw sequence reads were processed using the FastQC toolkit version 0.11.8 for quality control.[34] Adapter sequences and poor-quality reads were removed by the Trimgalore software version 0.6.6 (https://github.com/FelixKrueger/TrimGalore). 14–20 M quality filtered reads for each sample were obtained and mapped to reference genome GRCm38 using the Hisat2 software version 2.1.0.[29] Transcript-level expression analysis was performed with the StringTie software version 2.1.3[35] and the DESeq2 software version 1.30.0 (R package version 4.0)[32] to compute gene expression level and difference. P value < 0.05 and fold change >2 or fold change < 0.5 were set as the threshold for significantly differential expression.

Hierarchical cluster analysis of DEGs was performed to explore gene expression patterns. Gene ontology (GO) enrichment and Kyoto encyclopedia of genes and genomes (KEGG) pathway enrichment analysis of DEGs were respectively performed using the clusterProfiler R package (version 3.18.0), which can calculate *P* values of the statistically significant categories.[36] Transcription factor enrichment analysis was conducted using ChEA database through Enrichr website (https://maayanlab.cloud/Enrichr/) according to DEGs.

Sequencing data and raw counts are available in NCBI's Sequence Read Archive (SRA) database through SRA accession number PRJNA765909 (*Phactr1*$^{+/+}$ *vs. Phactr1*$^{-/-}$) and SRA accession number: PRJNA765919 (*Phactr1*^{ECKO}*Apoe*$^{-/-}$ *vs. Phactr1*$^{f/f}$*Apoe*$^{-/-}$).

Immunoprecipitation

Myc-tagged PPARγ overexpressing plasmid was purchased from Sino biological. cDNA for PHACTR1 isoform D was amplified from HUVECs and subcloned to pCMV-HA plasmid (Takara). PPARγ corepressor motif-mutated PHACTR1 plasmids were constructed by PCR amplification. Wild-type or mutated PHACTR1-overexpressing plasmids and PPARγ-overexpressing plasmids were transfected into 293FT using Lipofectamine 2000 Reagent (Thermo Fisher Scientific), and cells were harvested after 48 hours. As previously described,[37] lysates containing 800 μg soluble proteins were incubated with anti-HA or anti-Myc antibodies (diluted 1:50) overnight at 4°C. Antibody complexes were collected by incubation with Protein A/G agarose (Santa Cruz Biotechnology) for 4 hours at 4°C. Precipitates were washed 6 times with PBS, resuspended in SDS-PAGE loading buffer and boiled at 100°C for 10 minutes. After centrifugation at room temperature (14,000 rpm) for 5 minutes, protein extract supernatant was collected for western blot analysis.

PPARγ luciferase reporter assay

293FT cells were transfected with PHACTR1 and PPARγ plasmids, together with PPARγ Cignal Reporter plasmid (QIAGEN), using Lipofectamine 2000 Reagent (Thermo Fisher Scientific). After 48 hours, cells were treated with 10 μM pioglitazone for 12 hours and luciferase activity was measured by dual-luciferase reporter assay system (Promega).

For HUVEC, cells were transfected with PPARγ luciferase reporter lentivirus (Genomeditech) at an MOI of 25 at 24 hours after siRNA treatment. After another 24 hours, HUVECs were treated with different shear stress for 12 hours as mentioned above and luciferase activity was measured by dual-luciferase reporter assay system (Promega).

RNA interference (RNAi) experiments

PHACTR1 siRNA (siRNA ID: SASI_Hs01_00014343) and negative control siRNA were purchased from Sigma-Aldrich. HUVECs at 70% confluence in 35-mm dishes were transfected by 50 nM siRNA using Lipofectamine 2000 Reagent (Thermo Fisher Scientific). Four hours after transfection, medium was changed to fresh complete ECM, and cells were cultured for 48 hours before treatment.

In vitro monocyte adhesion assay

HUVECs were transfected with *PHACTR1* siRNA and control siRNA as aforesaid and stimulated with 2 ng/mL TNF-α for 16 hours. PBMCs were labeled for 30 minutes at 37°C with 10 μM BCECF-AM (Beyotime Biotechnology) in RPMI 1640 medium, and washed three times with PBS. Labeled PBMCs (10^6 cells/mL) were added to monolayers of siRNA-transfected HUVEC and incubated for 40 minutes. Non-adherent cells were removed by washing with PBS 4 times, and adherent cells were fixed with 4% PFA. Cells were stained with Hoechst33342 (Sigma-Aldrich) and attached cells were then observed by the IX83 inverted fluorescent microscope (Olympus). EC-monocyte adhesion was quantified by calculating the ratio of THP-1 or PBMC cell numbers to HUVEC numbers.

Statistical analysis

Data are presented with mean±SEM and statistical analyses were done using GraphPad Prism, version 7. The Shapiro-Wilk test was used to analyze data normality. For normally distributed data, comparisons between two groups were analyzed using the two-tailed Student's *t*-test (equal variance) or two-tailed Student's *t*-test with Welch's correction (unequal variance). Multiple comparisons were performed using repeated measures one-way ANOVA with the Greenhouse-Geisser correction followed by Dunnet's *post hoc* test or 2-way ANOVA followed by Bonferroni's *post hoc* test. For non-normally distributed data, non-parametric tests were employed. Mann-Whitney test was used for two-group analysis and multiple comparisons were performed using the Kruskal-Wallis test with Dunn's multiple comparisons test. A *P* value of less than 0.05 was considered significant.

RESULTS

Phactr1$^{-/-}$ mice had no apparent abnormities

We generated *Phactr1*$^{-/-}$ mice by deleting *Phactr1* exon 7 (ENSMUSE00000493553) using the CRISPR/Cas9 system (Figure 1A). The deletion caused the shifting of reading frames as well. Targeting of *Phactr1* was confirmed by genotyping using tail DNA and conventional PCR, as well as western blot of brains of *Phactr1*$^{-/-}$ mice and its littermate controls due to the highest expression being found in the brain (Figure 1B through 1D).

Phactr1$^{-/-}$ mice were born at the expected Mendelian ratio and were fertile (Table S1). Body weights were similar between knockout mice and wild-type mice (Figure 1E). The gross appearance of *Phactr1*$^{-/-}$ mice was normal, and no apparent abnormalities were observed (Figure 1F). *Phactr1* deficiency did not affect cardiac function determined by echocardiography and heart weight/tibial length ratio, while the systolic blood pressure was comparable between wild-type and knockout mice (Figure S1).

Global *Phactr1* deficiency attenuated the HF-HC diet-induced atherosclerosis in *Apoe*$^{-/-}$ mice

To determine the effect of *Phactr1* on atherosclerosis, we generated *Phactr1*$^{-/-}$*Apoe*$^{-/-}$ mice by breeding *Phactr1*$^{-/-}$ mice with *Apoe*$^{-/-}$ mice, the atheroprone mouse model. Since the associations of *PHACTR1* with CADs were mainly identified in elderly men and women (postmenopausal), we focused on male mice in this study. Eight-week-old

Phactr1$^{-/-}$*Apoe*$^{-/-}$ and *Phactr1*$^{+/+}$*Apoe*$^{-/-}$ mice were fed a HF-HC diet for 12 weeks to induce atherosclerosis. We then performed phenotypic characterization. Although PHACTR1 was highly expressed in the brain,[5] the body weights, the food intake, the weights of major organs including white adipose tissue, liver, spleen, lung, kidney, and heart, and the heart weight/tibia length ratios were similar between *Phactr1*$^{-/-}$*Apoe*$^{-/-}$ and *Phactr1*$^{+/+}$*Apoe*$^{-/-}$ mice (Figure S2).

Aortic atherosclerotic lesions were visualized by Masson's trichrome staining of the aortic sinus and *en face* oil red O staining of the whole aorta. Surprisingly, *Phactr1* deficiency significantly attenuated atherosclerosis in *Apoe*$^{-/-}$ mice (Figure 1G through 1L). Masson's trichrome staining showed that atherosclerotic plaque areas in the aortic sinus decreased by 22.3% in *Phactr1*$^{-/-}$*Apoe*$^{-/-}$ mice compared with *Phactr1*$^{+/+}$*Apoe*$^{-/-}$ mice (Figure 1G and 1H). *En face* oil red O staining showed that atherosclerotic lesion decreased by 27.00% in the aortic arch of *Phactr1*$^{-/-}$*Apoe*$^{-/-}$ mice compared with *Phactr1*$^{+/+}$*Apoe*$^{-/-}$ mice, but was comparable in the thoracic/abdominal aorta (Figure 1I through 1L). These findings indicate that PHACTR1 is required for the development of atherosclerosis.

PHACTR1 was highly expressed in murine ECs

The associations between SNP and gene expression, which are tissue- or cell-type-dependent, could be analyzed using the GTEx database. We searched the database (GTEx Analysis Release V8; dbGaP Accession phs000424.v8.p2) and found that the four *PHACTR1* SNPs (rs12526453, rs9349379, rs9369640, and rs4714955) were associated with *PHACTR1* mRNA expression and that the associations are mainly in non-diseased arteries (including tibial artery, aorta and coronary artery) but not in nervous system, immune system or other tissues among the 49 tissues analyzed (Figure 2A and Table S2), suggesting the effect of the vascular PHACTR1 on atherosclerosis.

Considering the inconsistency of mRNA and protein expression of genes, we depicted the PHACTR1 protein expression profile in *Phactr1*$^{+/+}$*Apoe*$^{-/-}$ mice and found that PHACTR1 was highly expressed in brain and lung while no specific PHACTR1 bands were detected in heart, liver, spleen, colon or adipose tissue (Figure 2B). Compared to previous reports,[13, 14] we found that PHACTR1 protein was undetectable in bone marrow tissues or bone marrow-derived macrophages of *Apoe*$^{-/-}$ mice (Figure 2C through 2E), possibly due to different genomic backgrounds of the mice (mice from Kasikara et al.: C57BL/6NCrl backcrossed with C57BL/6J for more than 10 generations; our mice: C57BL/6J).[38] In *in vivo* study, we always use littermate controls to eliminate the potential influence of genetic backgrounds. We also observed that PHACTR1 was expressed in the aorta, specifically restricted in the aortic intima (mainly ECs), but not in media (mainly vascular smooth muscle cells, VSMCs) and adventitia (Figure 2F and 2G). These data imply the potential role of endothelial PHACTR1 in the progression of atherosclerosis.

PHACTR1 has several isoforms. Human PHACTR1 has 13 transcript variants and 9 protein isoforms, while murine PHACTR1 has the orthologs of human isoform A, B and D. Isoform A (580 amino acids (Aas)) is the major isoform in the brain, while isoform D (557 Aas) is the dominant isoform in humans ECs and macrophages.[16] Although isoform A has more Aas than isoform D, its actual molecular weight (about 65kDa) is lower than isoform D

(about 70kDa), according to western blot results from us and Reschen *et al.*[16] Exon 7, which we deleted to generate *Phactr1*$^{-/-}$ mice, exists in almost all mouse isoforms, except isoform 3, the shortest mouse isoform without human orthologs (144 amino acids compared with 400–600 amino acids of other isoforms). Similar to prior human studies, we found that PHACTR1 isoform 4 (human isoform A ortholog) was prominently expressed in the mouse brain, and that PHACTR1 isoform 5 (human isoform D ortholog) was the major isoform expressed in aortic ECs and lung of mice (Figure 2B and 2F through 2H).

Endothelial *Phactr1* was required for atherosclerosis in disturbed flow regions of *Apoe*$^{-/-}$ mice

To specifically investigate the role of endothelial PHACTR1 in atherosclerosis, we generated EC-specific *Phactr1* knockout mice (*Phactr1*^{ECKO}) by breeding *Phactr1* floxed mice (*Phactr1*$^{f/f}$) with *Tie2*-Cre mice (Figure 3A). Although *Tie2* (encoded by *TEK* gene) promoters are partially activated in some hematopoietic cells besides ECs, there was no PHACTR1 expression in the macrophages of mice we used (Figure 2C through 2E). To further ensure the high specificity of *Phactr1* depletion in ECs, we chose the strain, B6.Cg-Tg(Tek-cre)1Ywa/J, which was proved to have much fewer Cre-positive blood cells (less than 5%) than other strains (over 82%).[39, 40] Considering abundant ECs in the lung (30–50%),[41] we determined pulmonary PHACTR1 protein expression to confirm the knockout of endothelial *Phactr1* in *Phactr1*^{ECKO} mice. Western blot showed that PHACTR1 expression decreased by 38.1% in lung tissues of *Phactr1*^{ECKO} mice compared with control *Phactr1*$^{f/f}$ mice (Figure S3).

After breeding with *Apoe*$^{-/-}$ mice, *Phactr1*^{ECKO}*Apoe*$^{-/-}$ and *Phactr1*$^{f/f}$*Apoe*$^{-/-}$ control mice were generated and fed with the HF-HC diet for 12 weeks starting from the age of 8 weeks. Atherosclerosis was analyzed as described above. Consistent with global knockout mice, atherosclerotic plaque areas in aortic roots decreased by 22.1% in *Phactr1*^{ECKO}*Apoe*$^{-/-}$ mice compared with littermate controls determined by oil red O staining (Figure 3B and 3C). *En face* staining showed that EC-specific *Phactr1* knockout significantly attenuated atherosclerosis in the aortic arch region but not in the thoracic/abdominal aorta (Figure 3D through 3G). Disturbed blood flow in the aortic arch promotes atherosclerotic plaque formation[42] and our results imply that endothelial PHACTR1 may mediate this process.

To further confirm the role of PHACTR1 in disturbed flow-related atherosclerosis, we performed a partial carotid ligation model in *Phactr1*^{ECKO}*Apoe*$^{-/-}$ and *Phactr1*$^{f/f}$*Apoe*$^{-/-}$ littermate control mice as previously described.[24, 43] To trigger oscillatory flow in the LCA, three branches of LCA (external carotid artery, internal carotid artery and occipital artery) were completely ligated and one branch (superior thyroid artery) was left open. After the surgery, mice were fed with the HF-HC diet for two weeks and atherosclerotic lesions in LCAs were analyzed (Figure 3H). Oil red O staining of frozen sections showed that EC-specific *Phactr1* knockout significantly attenuated disturbed flow-related atherosclerotic plaque formation by 58.5% (Figure 3I and 3J). Therefore, endothelial PHACTR1 can regulate disturbed flow-primed atherosclerosis.

Endothelial PHACTR1 was located in the nucleus under disturbed flow

To investigate the role of PHACTR1 in endothelial response to blood flow, we detected PHACTR1 expression in ECs stimulated by different shear stress. Surprisingly, EC PHACTR1 mRNA expression was not regulated by shear stress. *In vivo*, intimal *Phactr1* mRNA levels were comparable between sham-operated RCAs and ligated LCAs on day 3 after ligation, although the expression of *Klf2*, a well-characterized shear stress-sensitive gene, decreased remarkably under DF compared with LF (Figure 3K and 3L). *In vitro*, *PHACTR1* mRNA expression showed no difference in HUVECs under LF with high shear stress (12 dynes/cm^2) or under oscillatory DF (±6 dynes/cm^2, 1 Hz; Figure 3M and 3N).

PHACTR1 contains two nuclear localization signals and PHACTR1 (isoform A) exhibits nuclear accumulation transiently after FBS stimulation and returns to the cytosol after four hours in NIH-3T3 cells.[44] However, the localization of endothelial PHACTR1 (isoform D) is still unknown. Therefore, we studied the subcellular distribution of endothelial PHACTR1. Due to lack of commercially available functional antibodies for immunostaining, we transfected HUVECs with adenovirus to overexpress HA-tagged PHACTR1 isoform D (HA-PHACTR1-D), and detected PHACTR1 by immunofluorescence staining with anti-HA antibody. Surprisingly, PHACTR1 mainly localized in the cytosol under LF with high shear stress (12 dynes/cm^2) but was concentrated in the nucleus under oscillatory DF (±6 dynes/cm^2, 1 Hz; Figure 3O and 3P) or static conditions (Figure S4), which displays similar changes on inflammatory gene expression with DF compared to LF. These data suggested that laminar flow retained PHACTR1 in the cytosol while pro-atherogenic disturbed flow-induced PHACTR1 nuclear translocation.

Endothelial PHACTR1 was associated with vascular function and inflammation

To characterize the molecular function of endothelial PHACTR1, RNA-seq analysis was conducted using murine aortic ECs and we compared the gene expressions between *Phactr1*$^{-/-}$ and *Phactr1*$^{+/+}$ littermate control mice (n=3) or between *Phactr1*^{ECKO}*Apoe*$^{-/-}$ and *Phactr1*$^{f/f}$*Apoe*$^{-/-}$ littermates (n=4) respectively (Figure 4A). EC-enriched mRNA was extracted from aortas as previously described.[26, 27] Real-time PCR confirmed that extracted mRNA displayed high *Cdh5* (cadherin 5, an EC marker) expression and extremely low *Acta2* (coding gene of α-smooth muscle actin, a VSMC marker) expression compared to media and adventitia tissues (Figure 4B). Consistently, transcripts analysis showed that *Phactr1–206* (human PHACTR1 isoform D ortholog) was the main protein-coding transcript in ECs (Figure 4C).

The RNA-seq analysis yielded 191 DEGs (fold change>2, P value<0.05) in aortic ECs of *Phactr1*$^{-/-}$ mice compared with control mice with clustering of samples according to *Phactr1* genotype (Figure 4D). Functional annotation and enrichment analysis of DEGs were conducted to identify GO terms and KEGG pathways. KEGG pathway enriched in metabolism and inflammation-related pathway (Figure 4E and Table S3), while GO analysis highlighted biologic processes related to thermogenesis, vasculature development and immune response (Figure 4F and Table S4).

Gene expression in *Phactr1*^{ECKO}*Apoe*$^{-/-}$ and *Phactr1*$^{f/f}$*Apoe*$^{-/-}$ control mice was also analyzed. We modified the method using SMART-seq because of the low amounts of total RNA. Total 514 DEGs (fold change>2, *P* value<0.05) were revealed by SMART-seq (Figure 4G). Functional analysis demonstrated that deficiency of endothelial *Phactr1* mainly affected inflammation-related pathways (KEGG analysis; Figure 4H and Table S5) and changed biological processes related to vascular function and immune response (GO analysis; Figure 4I and Table S6). Therefore, integrating the bioinformatic analysis of DEGs from global and EC-specific *Phactr1* knockout ECs, we believed that endothelial PHACTR1 was involved in vascular function as well as inflammatory response.

PHACTR1 interacted with PPARγ and repressed PPARγ transcriptional activity

Considering the nuclear localization of PHACTR1, we further performed transcription factor binding motif overrepresentation analysis by oPOSSUM database[45] using DEGs from RNAseq to identify potential transcription factors associated with PHACTR1. Surprisingly, we found that PPARγ/retinoid X receptor α (RXRα) were the top-ranked overrepresented transcription factors with the highest *Z*-scores (*Z*-score=17.70, *Phactr1*$^{-/-}$ *vs. Phactr1*$^{+/+}$; *Z*-score=12.56, *Phactr1*^{ECKO}*Apoe*$^{-/-}$ *vs. Phactr1*$^{f/f}$*Apoe*$^{-/-}$; Figure 5A and 5B). Noteworthy, PPAR signaling was also highlighted in the corresponding KEGG analysis (Figure 4E). In the DEGs with potential PPARγ/RXRα binding sites, most genes were upregulated (*Phactr1*$^{-/-}$ *vs. Phactr1*$^{+/+}$: 42 of 66 genes; *Phactr1*^{ECKO}*Apoe*$^{-/-}$ *vs. Phactr1*$^{f/f}$*Apoe*$^{-/-}$: 181 of 232 genes; Figure 5C and 5D, Table S7 and Table S8), implying that absence of endothelial PHACTR1 increased PPARγ/RXRα transcriptional activity.

PPARγ is a member of ligand-dependent nuclear receptor superfamily, and forms a heterodimer with RXRα upon ligand binding and interacts with peroxisome proliferator responsive element in target genes to regulate gene transcription.[46, 47] To determine the function of PHACTR1 in PPARγ/RXRα-mediated transcription, the potential interactions among PHACTR1, PPARγ and RXRα were explored by co-immunoprecipitation. PHACTR1 was associated with PPARγ but not RXRα (Figure 5E and 5F), suggesting that PPARγ was the direct effector molecule of PHACTR1. Subsequently, the role of PHACTR1 in PPARγ signaling was analyzed. PPARγ transcriptional activity was measured in the presence or absence of PHACTR1 in 293FT cells, and the luciferase reporter assay showed that PHACTR1 overexpression significantly inhibited PPARγ agonist pioglitazone-induced activation by 33.2% (Figure 5G).

PPARγ transcription activity is precisely controlled by a series of coactivators and corepressors. The co-regulators bind to PPARγ ligand binding domains through highly conserved motifs, LXXLL motif for coactivators and LXXXIXXX(I/L) motif for corepressors.[48] PHACTR1 is evolutionarily conserved[49] and we analyzed the protein sequences from different species. Interestingly, human PHACTR1 contains two PPARγ corepressor motifs (LPSQIQHQL and LRQQIGTKL). PHACTR1 proteins of other species including mice, rats, chickens, and snakes share the second motif (LRQQIGTKL) with human PHACTR1, located in the highly conserved region. No corepressor motif exists in frogs or zebrafishes and no PPARγ coactivator motif was observed in PHACTR1 from any species (Figure 5H). Moreover, co-immunoprecipitation assay also showed that deletion

of both corepressor motifs in human PHACTR1 markedly reduced PHACTR1-PPARγ interaction (Figure 5I). All these results demonstrated that PHACTR1 was a potential PPARγ transcriptional corepressor by binding PPARγ through LXXXIXXX(I/L) motif.

PHACTR1 was required for EC activation and leukocyte adhesion under disturbed flow

PPARγ exhibited protective effects in atherosclerosis. Endothelial PPARγ attenuates atherosclerosis by trans-repressing NF-κB and AP-1, two critical inflammatory transcription factors, to reduce endothelial activation *in vitro* and *in vivo*.[50–52] Bioinformatic analysis also predicted the changes in inflammation processes after *Phactr1* knockout. Therefore, we speculated that PHACTR1 was critical for EC activation by inhibiting PPARγ activity in response to pro-atherosclerotic flow. *In vitro*, EC activation was evaluated after *PHACTR1* knockdown by specific siRNA (si*PHACTR1*) in HUVECs. PHACTR1 expression decreased by 61.4% at the mRNA level and by 72.2% at the protein level after siRNA transfection for 48 hours (Figure 6A through 6C). Under static conditions, real-time PCR and western blot results showed that *PHACTR1* depletion inhibited the mRNA and protein levels of VCAM-1 and ICAM-1 in HUVECs (Figure 6A through 6C). Furthermore, we treated cells with different shear stress as mentioned above, oscillatory DF (±6 dynes/cm^2, 1 Hz) or LF (12 dynes/cm^2). Compared with control siRNA, si*PHACTR1* reduced DF-induced VCAM-1 and ICAM-1 expression by 34.5% and 15.0% respectively, detected by immunofluorescence staining (Figure 6D and 6E), and inhibited DF-induced adhesion of PBMCs (peripheral blood mononuclear cells) to HUVECs by 63.8% (Figure 6F and 6G). Importantly, *PHACTR1* knockdown increased PPARγ transcriptional activity by 65.8% in HUVECs under DF (Figure 6H), and the reduction of VCAM-1 and ICAM-1 was restored by *PPARg* knockdown (Figure 6D and 6E), implying PHACTR1-mediated EC activation was through PPARγ inhibition.

In vivo, *en face* staining of mouse aortic arch revealed that endothelial VCAM-1 expression decreased significantly in disturbed flow regions of *Phactr1*$^{-/-}$ mice compared with wild-type littermates (Figure 6I and 6J). We also performed *in vivo* partial carotid ligation model in endothelial *Phactr1*-deficient mice. Three days after ligation, EC-enriched intimal mRNA was extracted from ligated LCA and sham-operated RCA (Figure 6K). Endothelial *Vcam1* and *Icam1* mRNA was determined by real-time PCR, and the ratios of mRNA in LCA to mRNA in RCA were calculated as previously described to assess the increment of gene expression after ligation.[24] In *Phactr1*$^{f/f}$ mice, the LCR/RCA ratios of *Vcam1* and *Icam1* mRNA were 3.45±0.62 and 2.52±0.53, respectively, while in *Phactr1*^{ECKO} mice the ratios were significantly decreased (*Vcam1*: 1.52±0.23, decreased by 55.9%, P=0.0189; *Icam1*: 1.03±0.12, decreased by 58.9%, P=0.0478; Figure 6L and 6M). Endothelial activation accelerated atherosclerosis by facilitating the recruitment of immune cells. CD68 staining showed that endothelial *Phactr1* depletion decreased macrophage infiltration by 65.0% in atherosclerotic lesions induced by partially ligating carotid artery in *Apoe*$^{-/-}$ mice (Figure 6N and 6O). These results suggested that endothelial PHACTR1 facilitated atherosclerosis progression by promoting inflammatory adhesion factor expression and subsequently leukocyte infiltration.

PPARγ antagonist GW9662 eliminated the protective effects of *Phactr1* depletion on endothelial activation and atherosclerosis *in vivo*

We further investigated whether the PHACTR1 mediated atherosclerosis through repressing PPARγ signaling *in vivo*. We performed partial carotid ligation on *Phactr1*^{ECKO}*Apoe*$^{-/-}$ and *Phactr1*$^{f/f}$*Apoe*$^{-/-}$ littermates followed by the HF-HC diet. All mice were treated with PPARγ antagonist GW9662 (3.6 μmol/kg body weight (1 mg/kg body weight), i.p.) once daily from pre-surgery day 2 to the day before euthanasia. Two weeks after the surgery, the ligated carotid arteries were harvested and analyzed (Figure 7A). With GW9662 administration, the atherosclerotic plaques were comparable between *Phactr1*^{ECKO}*Apoe*$^{-/-}$ and *Phactr1*$^{f/f}$*Apoe*$^{-/-}$ mice (Figure 7B and 7C), and CD68 positive macrophages showed no difference between the two groups (Figure 7D and 7E), suggesting that GW9662 diminished the protective effects of endothelial *Phactr1* knockout. Moreover, GW9662 treatment also eliminated the reduction of disturbed flow-induced *Vcam1* and *Icam1* expression caused by *Phactr1* depletion (both *Vcam1* and *Icam1* mRNA LCA/RCA ratios were comparable between *Phactr1*$^{f/f}$+GW9662 and *Phactr1*^{ECKO}+GW9662 groups; Figure 7F through 7H). These results demonstrated that PHACTR1 mediated EC activation and atherosclerosis by repressing PPARγ signaling.

DISCUSSION

The major finding of the current study is the *in vivo* pro-atherosclerotic properties of endothelial PHACTR1, which functions as a PPARγ transcription corepressor under disturbed flow (Figure 7I). *PHACTR1* is significantly associated with CAD according to several large-scale GWAS, and analysis of GTEx database demonstrates that these SNPs strongly associate *PHACTR1* gene expression in arteries. We generated *Phactr1* global and EC-specific KO mice to study its biological functions in the progression of atherosclerosis. Our results demonstrated that *Phactr1* deficiency inhibited EC activation and attenuated the HF-HC diet-induced atherosclerosis in disturbed flow regions of arteries. Mechanistically, PHACTR1 was located in the nucleus under disturbed flow, interacted with PPARγ as its transcriptional corepressor, and promoted the expression of adhesion molecules negatively regulated by PPARγ in ECs. We are the first to discover a pathological function of endothelial PHACTR1 in atherosclerosis *in vivo* and the related mechanisms.

GWAS has become a useful approach to find genetic variations associated with particular diseases, especially common and complex diseases, which contribute a lot to the discovery of novel biological mechanisms. Several SNPs at the *PHACTR1* locus were discovered to be significantly related to CAD, but biological interpretation for these variants is challenging. Gupta *et al* found that rs9349379 on *PHACTR1* was a distal regulator of endothelin-1 (encoded by *EDN1*),[53] but in our study neither RNA-seq nor qPCR analysis showed significant changes of endothelin-1 in aortic ECs after *Phactr1* knockout (Figure S5), which is consistent with other two studies.[19, 54] This may be explained by the location of rs9349379 (chr6: 12903725) since our knockout mice were generated by exon 7 (corresponding human exon position: chr6: 13205815–13206136) deletion, which did not affect rs9349379 site (upstream). On the other hand, eQTL analysis showed that CAD-related SNPs on *PHACTR1* including rs9349379 were all *cis*-eQTL for *PHACTR1*,

suggesting the synergistic effects of these SNPs on atherosclerosis are probably attributable to the biological functions of PHACTR1. Although combining GWAS and eQTL analysis provides clues about gene functions, there are still limitations. Gene expression effects of eQTLs could be in the opposite direction between different tissues[55] and G allele on rs9349379 is associated with low PHACTR1 expression in arteries but high expression in atrial appendage (Table S2). Moreover, most eQTL analyses did not take different mRNA isoforms into account. With all things considered, biological experiments are crucial to provide direct evidence of PHACTR1 effects on atherosclerosis.

We focused on the role of endothelial PHACTR1 in atherosclerosis for several reasons. In both human and mice, PHACTR1 mRNA expression is abundant in ECs according to our real-time PCR and RNA-seq data and prior reports.[16] Importantly, western blot showed that PHACTR1 protein was enriched in murine ECs but not in other vascular cell types such as VSMCs. Consistently, Reschen *et al* reported the expression of PHACTR1 in human ECs but not in VSMCs.[16] Moreover, PHACTR1 was undetectable in murine bone marrow-derived macrophages in our study. Therefore, we generated EC-specific *Phactr1* KO mice which resembled global KO mice showing similar anti-atherosclerotic effects. These results indicated the involvement of EC *Phactr1* in atherosclerosis. However, Kasikara *et al* recently reported that transplantation of *Phactr1*$^{-/-}$ (also deleting exon 7) bone marrow increased plaque necrosis in atherosclerotic lesions in *Ldlr*$^{-/-}$ mice.[14] The inconsistency implies the distinct roles of macrophage *Phactr1* versus endothelial *Phactr1* in atherosclerosis. Unfortunately, the effects of global *Phactr1* depletion on atherosclerosis were not reported in this study. In addition, Li *et al* reported that deleting *Phactr1* exon 2–3 led to more atherosclerotic lesions in *Apoe*$^{-/-}$ mice,[13] which is inconsistent with our data, but exon 2–3 is not included in the transcripts of isoform D ortholog (the major isoform in vascular cells) and this isoform could not be knocked out in these mice (Table S9). Therefore, the exacerbated atherosclerosis may reflect the functions of other minor isoforms.

Apoe$^{-/-}$ mice are a well-characterized atherosclerosis model by inducing hypercholesteremia. Our results showed that the anti-atherosclerosis effects of endothelial PHACTR1 are not due to the changes in lipid profile. Although global *Phactr1* knockout decreased plasma cholesterol by 13.7% (mainly VLDL) in *Apoe*$^{-/-}$ mice (Figure S6A and S6B), EC-specific *Phactr1* knockout had no effects (Figure S6E through S6G), suggesting that endothelial PHACTR1 was not involved in lipid metabolism. Future studies will explore the potential roles of PHACTR1 in cholesterol metabolism using tissue-specific *Phactr1* KO mice.

We demonstrated that PHACTR1 regulated PPARγ activity by direct interaction. Endothelial *Pparg* knockout mice have increased plasma fatty acid and triglyceride.[50, 56] But our results showed that *Phactr1* depletion did not affect the expression of lipid metabolic genes in aortic endothelial cells, including *Cd36*, *Fabp4* and *Gpihbp1* (Figure S6H through S6M). The differences in lipid profile in *Phactr1 and Pparg* EC knockout mice are possibly due to the distinct expression pattern of two proteins[57] or specific target genes of PHACTR1 and PPARγ complex (may involve different co-activators or co-repressors), since we also found that PHACTR1 did not interact with RXRα, the classical PPARγ cofactor involved in lipid metabolism. Besides lipid regulating functions, endothelial PPARγ inhibits

endothelial activation by trans-repressing NF-κB and AP-1.[51] Although Zhang *et al* showed the interaction among PHACTR1, NF-κB p65 and MRTF-A in ECs,[18] the effect of MRTF-A on inflammation was controversial.[58, 59] Moreover, our data demonstrated that PPARγ inhibition rescued the effects of PHACTR1 deficiency on inflammation and atherosclerosis. Therefore, endothelial PHACTR1-PPARγ complex in the nucleus promotes atherosclerosis by increasing inflammation under disturbed flow.

Mechanical stress from blood flow is crucial for the progression of atherosclerosis and mechanosensitive molecules, including PPARγ, have been promising therapeutic targets for atherosclerosis.[4, 60] Laminar flow induces PPARγ expression and augments the levels of epoxyeicosatrienoic acids, the ligand of PPARγ, to activate PPARγ transcriptional activity and exert anti-inflammatory effects in ECs.[61, 62] But the regulatory mechanism of PPARγ activity remains unclear under disturbed flow. Importantly, our data showed that endothelial PHACTR1 is a disturbed flow-specific regulator of PPARγ signaling, shuttling to the nucleus and interacting with PPARγ to repress its transcriptional activity under disturbed flow.

PHACTR1 displayed nuclear localization under disturbed flow and cytoplasmic distribution under laminar flow and the mechanism of PHACTR1 shuttling is still unexplored. Wiezlak *et al* reported PHACTR1 nuclear import can be induced by G-F transformation of actin and RhoA activation under FBS stimulation in NIH-3T3 cells.[44] Disturbed flow with low shear stress can also activate RhoA kinase in ECs[63] and may subsequently induce PHACTR1 shuttling to the nucleus. Further investigation is needed in future studies.

PP1 is another PHACTR1 interacting protein and PHACTR1 is named as the regulator of PP1 activity by directly binding PP1 through its C terminus.[5] Although PP1 inhibits inflammation through dephosphorylating eIF2α[64] or TAK1[65] in immune cells, these reactions happen in the cytosol, and aforementioned studies gave opposite conclusions on the regulation of PHACTR1 to PP1 activity.[5, 49] But our RNA-seq data and rescue experiments demonstrated that PPARγ was the direct effector of endothelial PHACTR1. More comprehensive investigation of PHACTR1 functions and mechanisms is needed in the future.

In summary, we have demonstrated that endothelial PHACTR1 is a novel pro-atherosclerotic molecule by regulating endothelial cell activation as a transcriptional corepressor of PPARγ under disturbed flow. PPARγ is an ideal therapeutic target, and PPARγ agonists have emerged as protectors for endothelial function besides metabolic actions.[66, 67] However, adverse effects such as heart failure and liver dysfunction were observed because of the universal expression and diverse functions of PPARγ. Therefore, interrupting the association of endothelial PHACTR1 and PPARγ using small peptides or molecules could be a promising therapeutic strategy in diseases such as atherosclerosis.

Supplementary Material

Refer to Web version on PubMed Central for supplementary material.

Acknowledgments

We thank Prof. Hanjoong Jo (Georgia Institute of Technology and Emory University) for generous advice on the partial ligation model, Yudong Zhou and Dr. Junfeng Shi (Shanghai Jiao Tong University) for assistance in bioinformatics analysis, Dr. Wenhui Yue for advice on FACS analysis, Dr. Wen Su (Shenzhen University) for advice on PPARγ activity detection, Sujing Qiang and Shaobo Xue for assistance in animal experiments and Tiffany Nguyen for editing the manuscript.

Sources of Funding

This work was supported by the National Natural Science Foundation of China (grant 82270414 and grant 81700431 to D.J.), the Shanghai Science and Technology Committee (grant 21S11902900 to D.J.), the Ministry of Science and Technology of China project (grant 2017YFC0111800 to Y.X.), the China Postdoctoral Science Foundation (grant 2018M642090 to D.J.) and National Institutes of Health (grant HL084312 to E.A.F.).

Nonstandard Abbreviations and Acronyms

CAD	coronary artery disease
DEG	differentially expressed gene
DF	disturbed flow
EC	endothelial cell
eQTL	expression quantitative trait loci
FBS	fetal bovine serum
FPKM	Fragments Per Kilobase of exon model per Million mapped fragments
GO	gene ontology
GTEx	Genotype-Tissue Expression project
GWAS	genome-wide association study
HF-HC	high-fat, high-cholesterol
HUVEC	human umbilical vein endothelial cell
ICAM-1	intercellular cell adhesion molecule 1
KEGG	Kyoto encyclopedia of genes and genomes
LCA	left carotid artery
LF	laminar flow
PBMC	peripheral blood mononuclear cells
PHACTR1	phosphatase and actin regulator 1
PP1	protein phosphatase 1
PPARγ	peroxisome proliferator-activated receptor gamma

RCA	right carotid artery
RNA-seq	RNA sequencing
RXRα	retinoid X receptor α
sgRNA	small guide RNA
SRA	NCBI's Sequence Read Archive database
VCAM-1	vascular cell adhesion molecule 1
VSMC	vascular smooth muscle cell

REFERENCES

1. Libby P, Ridker PM, Hansson GK. Progress and challenges in translating the biology of atherosclerosis. Nature 2011;473:317–325 [PubMed: 21593864]
2. Zhou J, Li YS, Chien S. Shear stress-initiated signaling and its regulation of endothelial function. Arteriosclerosis, thrombosis, and vascular biology 2014;34:2191–2198 [PubMed: 24876354]
3. Heo KS, Fujiwara K, Abe J. Shear stress and atherosclerosis. Molecules and cells 2014;37:435–440 [PubMed: 24781409]
4. Qu D, Wang L, Huo M, Song W, Lau CW, Xu J, et al. Focal tlr4 activation mediates disturbed flow-induced endothelial inflammation. Cardiovascular research 2020;116:226–236 [PubMed: 30785200]
5. Allen PB, Greenfield AT, Svenningsson P, Haspeslagh DC, Greengard P. Phactrs 1–4: A family of protein phosphatase 1 and actin regulatory proteins. Proceedings of the National Academy of Sciences of the United States of America 2004;101:7187–7192 [PubMed: 15107502]
6. O'Donnell CJ, Kavousi M, Smith AV, Kardia SL, Feitosa MF, Hwang SJ, et al. Genome-wide association study for coronary artery calcification with follow-up in myocardial infarction. Circulation 2011;124:2855–2864 [PubMed: 22144573]
7. Lu X, Wang L, Chen S, He L, Yang X, Shi Y, et al. Genome-wide association study in han chinese identifies four new susceptibility loci for coronary artery disease. Nature genetics 2012;44:890–894 [PubMed: 22751097]
8. Myocardial Infarction Genetics C, Kathiresan S, Voight BF, Purcell S, Musunuru K, Ardissino D, et al. Genome-wide association of early-onset myocardial infarction with single nucleotide polymorphisms and copy number variants. Nature genetics 2009;41:334–341 [PubMed: 19198609]
9. Schunkert H, Konig IR, Kathiresan S, Reilly MP, Assimes TL, Holm H, et al. Large-scale association analysis identifies 13 new susceptibility loci for coronary artery disease. Nature genetics 2011;43:333–338 [PubMed: 21378990]
10. Consortium CAD, Deloukas P, Kanoni S, Willenborg C, Farrall M, Assimes TL, et al. Large-scale association analysis identifies new risk loci for coronary artery disease. Nature genetics 2013;45:25–33 [PubMed: 23202125]
11. Dichgans M, Malik R, Konig IR, Rosand J, Clarke R, Gretarsdottir S, et al. Shared genetic susceptibility to ischemic stroke and coronary artery disease: A genome-wide analysis of common variants. Stroke 2014;45:24–36 [PubMed: 24262325]
12. e GP. Enhancing gtex by bridging the gaps between genotype, gene expression, and disease. Nature genetics 2017;49:1664–1670 [PubMed: 29019975]
13. Li T, Ding L, Wang Y, Yang O, Wang S, Kong J. Genetic deficiency of phactr1 promotes atherosclerosis development via facilitating m1 macrophage polarization and foam cell formation. Clinical science 2020;134:2353–2368 [PubMed: 32857129]
14. Kasikara C, Schilperoort M, Gerlach B, Xue C, Wang X, Zheng Z, et al. Deficiency of macrophage phactr1 impairs efferocytosis and promotes atherosclerotic plaque necrosis. The Journal of clinical investigation 2021;131

15. Beaudoin M, Gupta RM, Won HH, Lo KS, Do R, Henderson CA, et al. Myocardial infarction-associated snp at 6p24 interferes with mef2 binding and associates with phactr1 expression levels in human coronary arteries. Arteriosclerosis, thrombosis, and vascular biology 2015;35:1472–1479 [PubMed: 25838425]
16. Reschen ME, Lin D, Chalisey A, Soilleux EJ, O'Callaghan CA. Genetic and environmental risk factors for atherosclerosis regulate transcription of phosphatase and actin regulating gene phactr1. Atherosclerosis 2016;250:95–105 [PubMed: 27187934]
17. Jarray R, Pavoni S, Borriello L, Allain B, Lopez N, Bianco S, et al. Disruption of phactr-1 pathway triggers pro-inflammatory and pro-atherogenic factors: New insights in atherosclerosis development. Biochimie 2015;118:151–161 [PubMed: 26362351]
18. Zhang Z, Jiang F, Zeng L, Wang X, Tu S. Phactr1 regulates oxidative stress and inflammation to coronary artery endothelial cells via interaction with nf-kappab/p65. Atherosclerosis 2018;278:180–189 [PubMed: 30293016]
19. Rubin S, Bougaran P, Martin S, Abelanet A, Delobel V, Pernot M, et al. Phactr-1 (phosphatase and actin regulator 1) deficiency in either endothelial or smooth muscle cells does not predispose mice to nonatherosclerotic arteriopathies in 3 transgenic mice. Arteriosclerosis, thrombosis, and vascular biology 2022:101161ATVBAHA122317431
20. Wood A, Antonopoulos A, Chuaiphichai S, Kyriakou T, Diaz R, Al Hussaini A, et al. Phactr1 modulates vascular compliance but not endothelial function: A translational study. Cardiovascular research 2022
21. Jiang D, Ge J, Liao Q, Ma J, Liu Y, Huang J, et al. Igg and iga with potential microbial-binding activity are expressed by normal human skin epidermal cells. International journal of molecular sciences 2015;16:2574–2590 [PubMed: 25625513]
22. Daugherty A, Tall AR, Daemen M, Falk E, Fisher EA, Garcia-Cardena G, et al. Recommendation on design, execution, and reporting of animal atherosclerosis studies: A scientific statement from the american heart association. Arteriosclerosis, thrombosis, and vascular biology 2017;37:e131–e157 [PubMed: 28729366]
23. Bi X, Stankov S, Lee PC, Wang Z, Wu X, Li L, et al. Ilrun promotes atherosclerosis through lipid-dependent and lipid-independent factors. Arteriosclerosis, thrombosis, and vascular biology 2022;42:1139–1151 [PubMed: 35861973]
24. Nam D, Ni CW, Rezvan A, Suo J, Budzyn K, Llanos A, et al. Partial carotid ligation is a model of acutely induced disturbed flow, leading to rapid endothelial dysfunction and atherosclerosis. American journal of physiology. Heart and circulatory physiology 2009;297:H1535–1543 [PubMed: 19684185]
25. Garin G, Abe J, Mohan A, Lu W, Yan C, Newby AC, et al. Flow antagonizes tnf-alpha signaling in endothelial cells by inhibiting caspase-dependent pkc zeta processing. Circulation research 2007;101:97–105 [PubMed: 17525369]
26. Xu S, Koroleva M, Yin M, Jin ZG. Atheroprotective laminar flow inhibits hippo pathway effector yap in endothelial cells. Translational research : the journal of laboratory and clinical medicine 2016;176:18–28 e12 [PubMed: 27295628]
27. Nam D, Ni CW, Rezvan A, Suo J, Budzyn K, Llanos A, et al. A model of disturbed flow-induced atherosclerosis in mouse carotid artery by partial ligation and a simple method of rna isolation from carotid endothelium. Journal of visualized experiments : JoVE 2010
28. Patel RK, Jain M. Ngs qc toolkit: A toolkit for quality control of next generation sequencing data. PloS one 2012;7:e30619 [PubMed: 22312429]
29. Kim D, Langmead B, Salzberg SL. Hisat: A fast spliced aligner with low memory requirements. Nature methods 2015;12:357–360 [PubMed: 25751142]
30. Anders S, Pyl PT, Huber W. Htseq--a python framework to work with high-throughput sequencing data. Bioinformatics 2015;31:166–169 [PubMed: 25260700]
31. Roberts A, Trapnell C, Donaghey J, Rinn JL, Pachter L. Improving rna-seq expression estimates by correcting for fragment bias. Genome biology 2011;12:R22 [PubMed: 21410973]
32. Simon Anders WH. Differential expression of rna-seq data at the gene level - the deseq package 2012

33. Picelli S, Faridani OR, Bjorklund AK, Winberg G, Sagasser S, Sandberg R. Full-length rna-seq from single cells using smart-seq2. Nature protocols 2014;9:171–181 [PubMed: 24385147]
34. Chen S, Zhou Y, Chen Y, Gu J. Fastp: An ultra-fast all-in-one fastq preprocessor. Bioinformatics 2018;34:i884–i890 [PubMed: 30423086]
35. Pertea M, Pertea GM, Antonescu CM, Chang TC, Mendell JT, Salzberg SL. Stringtie enables improved reconstruction of a transcriptome from rna-seq reads. Nature biotechnology 2015;33:290–295
36. Yu G, Wang LG, Han Y, He QY. Clusterprofiler: An r package for comparing biological themes among gene clusters. Omics : a journal of integrative biology 2012;16:284–287 [PubMed: 22455463]
37. Jiang D, Zhuang J, Peng W, Lu Y, Liu H, Zhao Q, et al. Phospholipase cgamma1 mediates intima formation through akt-notch1 signaling independent of the phospholipase activity. Journal of the American Heart Association 2017;6
38. Mekada K, Yoshiki A. Substrains matter in phenotyping of c57bl/6 mice. Experimental animals 2021;70:145–160 [PubMed: 33441510]
39. Payne S, De Val S, Neal A. Endothelial-specific cre mouse models. Arteriosclerosis, thrombosis, and vascular biology 2018;38:2550–2561 [PubMed: 30354251]
40. Kisanuki YY, Hammer RE, Miyazaki J, Williams SC, Richardson JA, Yanagisawa M. Tie2-cre transgenic mice: A new model for endothelial cell-lineage analysis in vivo. Developmental biology 2001;230:230–242 [PubMed: 11161575]
41. Donati Y, Blaskovic S, Ruchonnet-Metrailler I, Lascano Maillard J, Barazzone-Argiroffo C. Simultaneous isolation of endothelial and alveolar epithelial type i and type ii cells during mouse lung development in the absence of a transgenic reporter. American journal of physiology. Lung cellular and molecular physiology 2020;318:L619–L630 [PubMed: 32022591]
42. VanderLaan PA, Reardon CA, Getz GS. Site specificity of atherosclerosis: Site-selective responses to atherosclerotic modulators. Arteriosclerosis, thrombosis, and vascular biology 2004;24:12–22 [PubMed: 14604830]
43. Zhang C, Zhou T, Chen Z, Yan M, Li B, Lv H, et al. Coupling of integrin alpha5 to annexin a2 by flow drives endothelial activation. Circulation research 2020;127:1074–1090 [PubMed: 32673515]
44. Wiezlak M, Diring J, Abella J, Mouilleron S, Way M, McDonald NQ, et al. G-actin regulates the shuttling and pp1 binding of the rpel protein phactr1 to control actomyosin assembly. Journal of cell science 2012;125:5860–5872 [PubMed: 22976292]
45. Ho Sui SJ, Mortimer JR, Arenillas DJ, Brumm J, Walsh CJ, Kennedy BP, et al. Opossum: Identification of over-represented transcription factor binding sites in co-expressed genes. Nucleic acids research 2005;33:3154–3164 [PubMed: 15933209]
46. Ahmadian M, Suh JM, Hah N, Liddle C, Atkins AR, Downes M, et al. Ppargamma signaling and metabolism: The good, the bad and the future. Nature medicine 2013;19:557–566
47. Finck BN. The ppar regulatory system in cardiac physiology and disease. Cardiovascular research 2007;73:269–277 [PubMed: 17010956]
48. Rosenfeld MG, Glass CK. Coregulator codes of transcriptional regulation by nuclear receptors. The Journal of biological chemistry 2001;276:36865–36868 [PubMed: 11459854]
49. Allain B, Jarray R, Borriello L, Leforban B, Dufour S, Liu WQ, et al. Neuropilin-1 regulates a new vegf-induced gene, phactr-1, which controls tubulogenesis and modulates lamellipodial dynamics in human endothelial cells. Cellular signalling 2012;24:214–223 [PubMed: 21939755]
50. Qu A, Shah YM, Manna SK, Gonzalez FJ. Disruption of endothelial peroxisome proliferator-activated receptor gamma accelerates diet-induced atherogenesis in ldl receptor-null mice. Arteriosclerosis, thrombosis, and vascular biology 2012;32:65–73 [PubMed: 22015658]
51. Ricote M, Glass CK. Ppars and molecular mechanisms of transrepression. Biochimica et biophysica acta 2007;1771:926–935 [PubMed: 17433773]
52. Li AC, Brown KK, Silvestre MJ, Willson TM, Palinski W, Glass CK. Peroxisome proliferator-activated receptor gamma ligands inhibit development of atherosclerosis in ldl receptor-deficient mice. The Journal of clinical investigation 2000;106:523–531 [PubMed: 10953027]

53. Gupta RM, Hadaya J, Trehan A, Zekavat SM, Roselli C, Klarin D, et al. A genetic variant associated with five vascular diseases is a distal regulator of endothelin-1 gene expression. Cell 2017;170:522–533 e515 [PubMed: 28753427]
54. Wang X, Musunuru K. Confirmation of causal rs9349379- phactr1 expression quantitative trait locus in human-induced pluripotent stem cell endothelial cells. Circulation. Genomic and precision medicine 2018;11:e002327 [PubMed: 30354304]
55. Mizuno A, Okada Y. Biological characterization of expression quantitative trait loci (eqtls) showing tissue-specific opposite directional effects. European journal of human genetics : EJHG 2019;27:1745–1756 [PubMed: 31296926]
56. Abumrad NA, Cabodevilla AG, Samovski D, Pietka T, Basu D, Goldberg IJ. Endothelial cell receptors in tissue lipid uptake and metabolism. Circulation research 2021;128:433–450 [PubMed: 33539224]
57. Kalucka J, de Rooij L, Goveia J, Rohlenova K, Dumas SJ, Meta E, et al. Single-cell transcriptome atlas of murine endothelial cells. Cell 2020;180:764–779 e720 [PubMed: 32059779]
58. Hayashi K, Murai T, Oikawa H, Masuda T, Kimura K, Muehlich S, et al. A novel inhibitory mechanism of mrtf-a/b on the icam-1 gene expression in vascular endothelial cells. Scientific reports 2015;5:10627 [PubMed: 26024305]
59. Fang F, Yang Y, Yuan Z, Gao Y, Zhou J, Chen Q, et al. Myocardin-related transcription factor a mediates oxldl-induced endothelial injury. Circulation research 2011;108:797–807 [PubMed: 21330600]
60. Niu N, Xu S, Xu Y, Little PJ, Jin ZG. Targeting mechanosensitive transcription factors in atherosclerosis. Trends in pharmacological sciences 2019;40:253–266 [PubMed: 30826122]
61. Liu Y, Zhu Y, Rannou F, Lee TS, Formentin K, Zeng L, et al. Laminar flow activates peroxisome proliferator-activated receptor-gamma in vascular endothelial cells. Circulation 2004;110:1128–1133 [PubMed: 15313948]
62. Liu Y, Zhang Y, Schmelzer K, Lee TS, Fang X, Zhu Y, et al. The antiinflammatory effect of laminar flow: The role of ppargamma, epoxyeicosatrienoic acids, and soluble epoxide hydrolase. Proceedings of the National Academy of Sciences of the United States of America 2005;102:16747–16752 [PubMed: 16267130]
63. Miyazaki T, Honda K, Ohata H. M-calpain antagonizes rhoa overactivation and endothelial barrier dysfunction under disturbed shear conditions. Cardiovascular research 2010;85:530–541 [PubMed: 19752040]
64. Clavarino G, Claudio N, Dalet A, Terawaki S, Couderc T, Chasson L, et al. Protein phosphatase 1 subunit ppp1r15a/gadd34 regulates cytokine production in polyinosinic:Polycytidylic acid-stimulated dendritic cells. Proceedings of the National Academy of Sciences of the United States of America 2012;109:3006–3011 [PubMed: 22315398]
65. Gu M, Ouyang C, Lin W, Zhang T, Cao X, Xia Z, et al. Phosphatase holoenzyme pp1/gadd34 negatively regulates tlr response by inhibiting tak1 serine 412 phosphorylation. Journal of immunology 2014;192:2846–2856
66. Duan SZ, Usher MG, Mortensen RM. Peroxisome proliferator-activated receptor-gamma-mediated effects in the vasculature. Circulation research 2008;102:283–294 [PubMed: 18276926]
67. Wang XL, Oosterhof J, Duarte N. Peroxisome proliferator-activated receptor gamma c161-->t polymorphism and coronary artery disease. Cardiovascular research 1999;44:588–594 [PubMed: 10690291]

Highlights

- Analysis from GTEx database demonstrates that CAD-related SNPs at *PHACTR1* locus are correlated with *PHACTR1* mRNA expression in non-diseased artery tissues, suggesting the crucial role of *PHACTR1* in CAD.
- Both global and endothelial cell-specific *Phactr1* deficiency decrease atherosclerotic plaque formation in disturbed flow region of arteries from *Apoe*$^{-/-}$ mice.
- Nuclear PHACTR1 functions as an EC-specific PPARγ transcriptional corepressor to promote endothelial activation in response to disturbed flow.
- Drugs targeting PHACTR1 should be delivered cell-specifically due to the opposite effects of PHACTR1 in endothelial cells and macrophages.

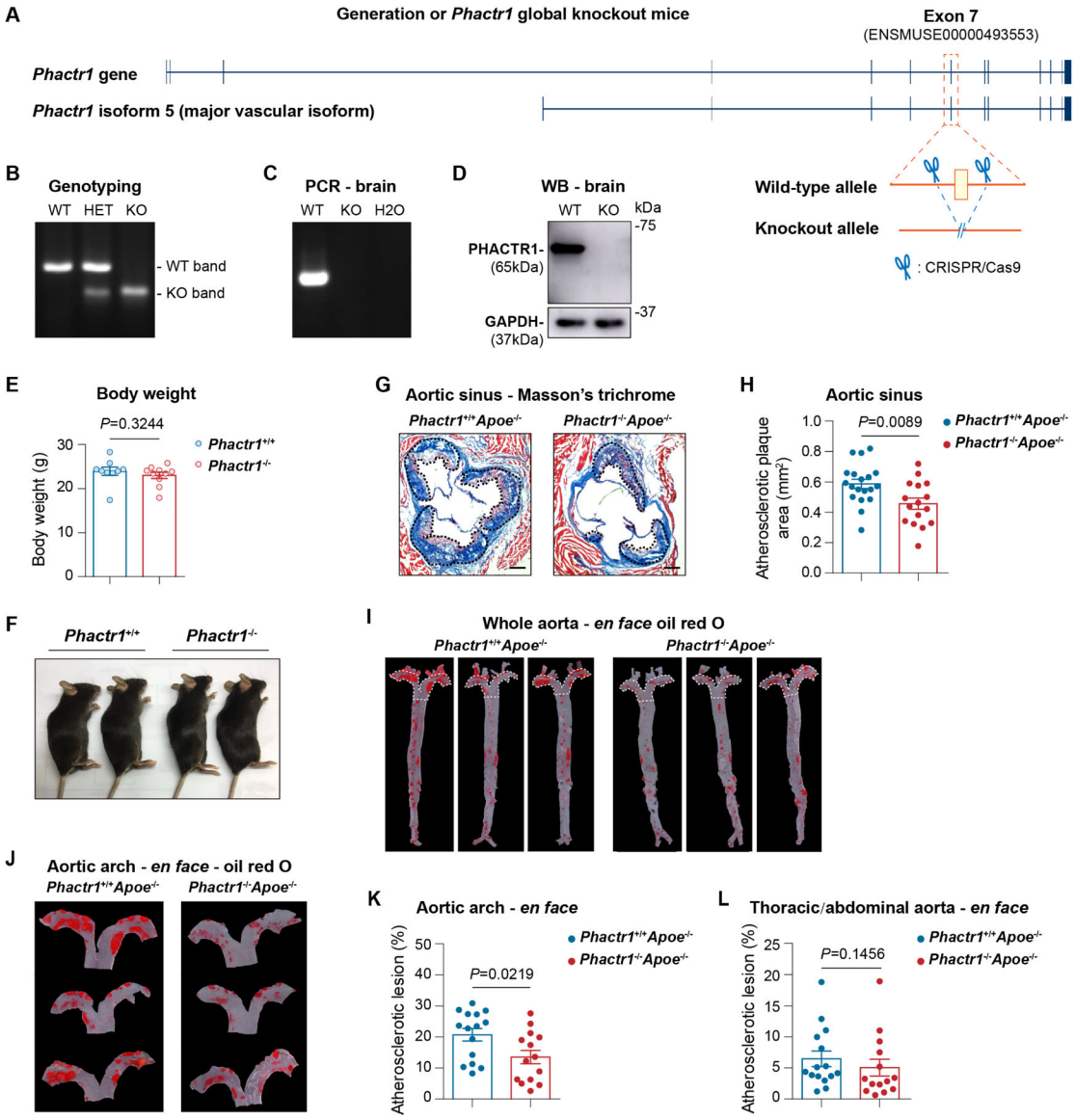

Figure 1. Global *Phactr1* knockout attenuated atherosclerosis in *Apoe*$^{-/-}$ mice.

A, *Phactr1* knockout (KO) mice were generated by deleting exon 7 using CRISPR/Cas9 system. **B** through **D**, Identification of *Phactr1* knockout (KO) mice by genotyping tail DNA (**B**) and detecting *Phactr1* exon 7 mRNA by PCR (**C**) and brain PHACTR1 protein (**D**) by immunoblot analysis of wild-type (WT) and KO mice. HET: heterozygous, WB: western blot. **E** and **F**, Body weights and gross appearance of WT and KO littermate mice of eight-week-old (n=9–11). **G** through **L**, Atherosclerotic lesions in the aortic sinus (Masson's trichrome staining, **G** and **H**) and in *en face* prepared aortas (oil red O staining, **I** through **L**) in *Phactr1*$^{-/-}$*Apoe*$^{-/-}$ and *Phactr1*$^{+/+}$*Apoe*$^{-/-}$ mice fed a HF-HC diet for 12 weeks (n=14–20). Scale bars: 200 μm. Data were presented as mean±SEM and analyzed using Mann-Whitney test in **E** and **L**, and unpaired two-tailed Student's t-test in **H** and **K**.

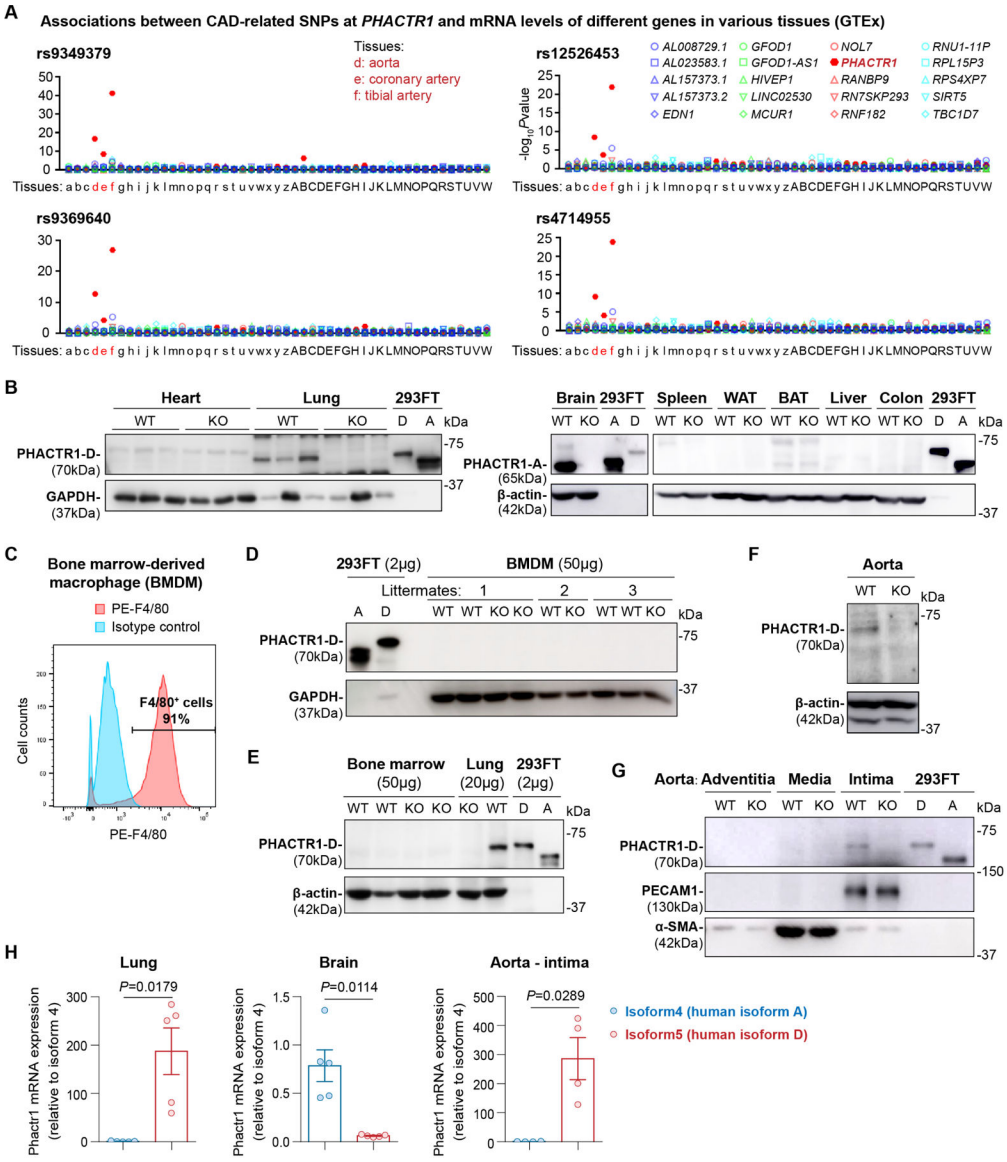

Figure 2. PHACTR1 expression was enriched in murine ECs, mainly as isoform 5 (human isoform D ortholog).

A, CAD-related SNPs in *PHACTR1* are cis-eQTLs for *PHACTR1* in arteries. Correlated genes of rs9349379, rs12526453, rs9369640, and rs4714955 in human tissues according to GTEx database. a: adipose (subcutaneous), b: adipose (omentum), c: adrenal gland, d: aorta, e: coronary artery, f: tibial artery, g: amygdala, h: brain (anterior cingulate cortex), i: caudate, j: cerebellar hemisphere, k: cerebellum, l: brain (cortex), m: brain (frontal cortex), n: hippocampus, o: hypothalamus, p: nucleus accumbens, q: putamen, r: spinal cord, cervical c-1, s: substantia nigra, t: mammary tissue, u: cultured fibroblasts, v: EBV transformed lymphocytes, w: sigmoid colon, x: transverse colon, y: gastroesophageal junction, z: esophagus (mucosa), A: esophagus (muscularis), B: heart (atrial appendage), C: heart (left ventricle), D: kidney, E: liver, F: lung, G: minor salivary gland, H: skeletal muscle, I: tibial nerve, J: ovary, K: pancreas, L: pituitary, M: prostate, N: skin (suprapubic), O: skin (lower leg), P: small intestine, Q: spleen, R: stomach, S: testis, T: thyroid, U: uterus, V: vagina, W:

whole blood. **B** through **G**, Immunoblot analysis of PHACTR1 protein in different tissues and cells of *Phactr1*$^{-/-}$*Apoe*$^{-/-}$ (KO) and *Phactr1*$^{+/+}$*Apoe*$^{-/-}$ (WT) mice. 293T with human PHACTR1 isoform A (PHACTR1-A or A) or D (PHACTR1-D or D) overexpression was used as positive control. Bone marrow-derived macrophages (BMDMs) were identified by FACS using PE-conjugated anti-F4/80 antibody (**C**). WAT: white adipose tissue, BAT: brown adipose tissue. **H**, mRNA expression of *Phactr1* isoform 4 and 5 in lung, brain and aorta tissues detected by real-time PCR. n=4–5. Data were presented as mean±SEM and analyzed using unpaired two-tailed Student's t-test with Welch's correction.

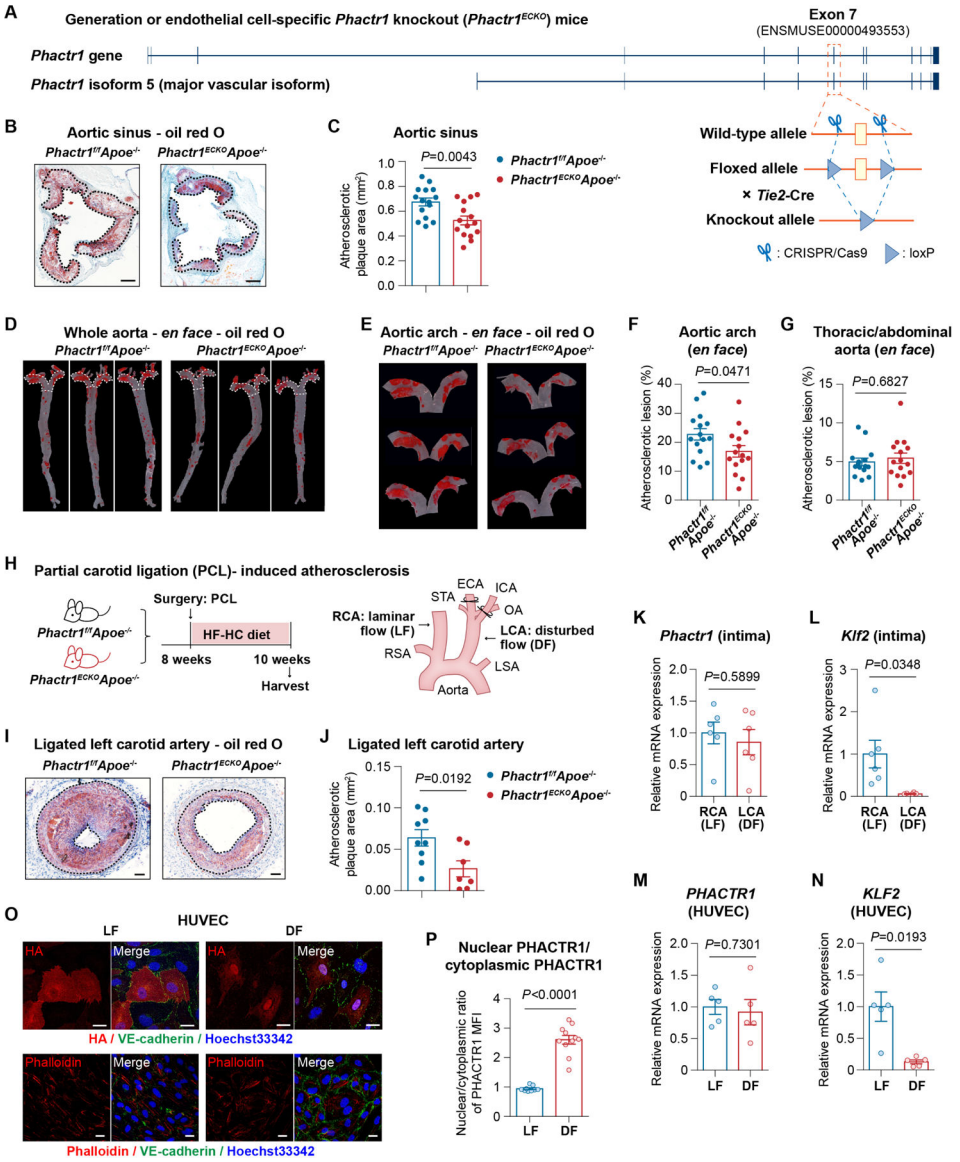

Figure 3. Loss of endothelial *Phactr1* attenuated atherosclerosis in disturbed flow regions of *Apoe*$^{-/-}$ mice.

A, EC-specific *Phactr1* KO mice were generated by crossing *Phactr1* floxed mice (loxP sites flanking exon 7 of *Phactr1*) with *Tie2*-Cre mice. **B** through **G**, Atherosclerosis was induced by 12 weeks of a HF-HC diet in *Phactr1*^{ECKO}*Apoe*$^{-/-}$ and *Phactr1*$^{f/f}$*Apoe*$^{-/-}$ littermates (n=15). Atherosclerotic lesions in aortic sinus (**B** and **C**) and in *en face* prepared aorta (**D** through **G**) were analyzed by oil red O staining in mice after feeding the HF-HC diet for 12 weeks. Scale bars: 200 μm. **H**, Partial carotid ligation was performed in *Phactr1*^{ECKO}*Apoe*$^{-/-}$ and *Phactr1*$^{f/f}$*Apoe*$^{-/-}$ mice (littermates), followed by a HF-HC diet for two weeks. RCA: left carotid artery, LCA: right carotid artery, RSA: right subclavian artery, LSA: left subclavian artery, STA: superior thyroid artery, ECA: external carotid artery, ICA: internal carotid artery, OA: occipital artery. **I** and **J**, Atherosclerotic lesions were analyzed by oil red O staining and quantified in frozen section of ligated carotid arteries at post-surgery day 14. Scale bars: 50 μm. n=7–8. **K** and **L**, Endothelial *Phactr1*

and *Klf2* mRNA expressions were determined by real-time PCR in partially ligated carotid arteries (n=6). Partial ligation models were performed and intimal RNA was collected from left carotid artery (LCA) and right carotid artery (RCA) 3 days after surgery. **M** and **N**, *PHACTR1* and *KLF2* mRNA was determined by real-time PCR in HUVECs treated with disturbed flow (DF, ±6 dyne/cm^2, 1Hz) or laminar flow (LF, 12 dyne/cm^2) for 24 hours. n=5. **O**, Localization of overexpressed PHACTR1 isoform D (HA-tagged) in HUVECs treated DF or LF for 6 hours, determined by immunofluorescence staining using anti-HA antibody. Scale bars: 20 μm. **P**, The subcellular distribution of PHACTR1 was quantified by nuclear/cytoplasmic ratios of PHACTR1 mean fluorescence intensity (MFI). n=9–11 cells from three independent experiments. Data were presented as mean±SEM and analyzed using unpaired two-tailed Student's t-test without correction in **C**, **F**, **J**, **K** and **M** and with Welch's correction in **L** and **N**, and Mann-Whitney test in **G** and **P**.

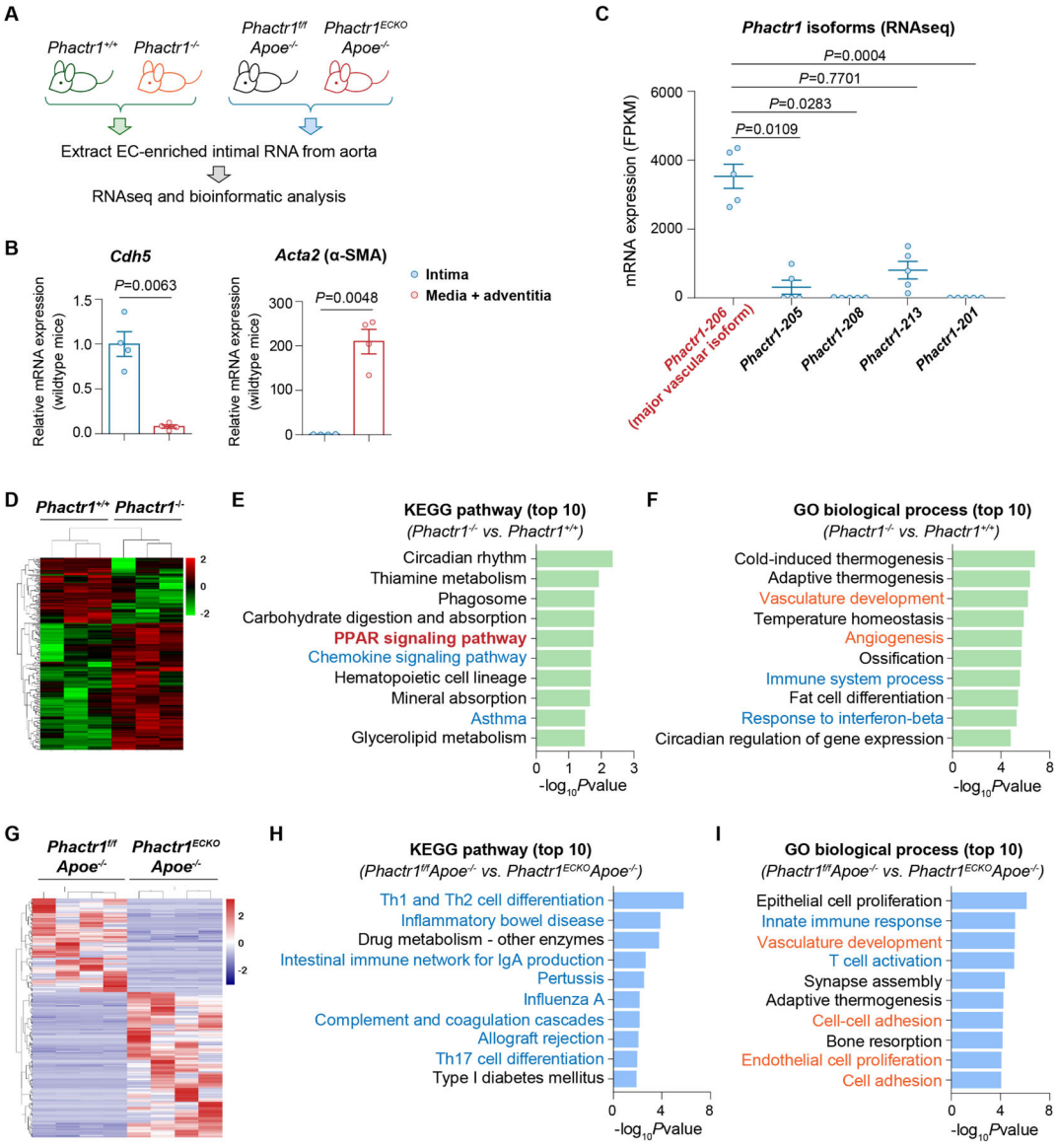

Figure 4. RNA-seq and bioinformatic analysis showed that endothelial PHACTR1 was related to vascular function and inflammatory response.

A, EC-enriched intimal mRNA was extracted from aortas of *Phactr1*$^{-/-}$ and *Phactr1*$^{+/+}$ littermate control mice (n=3) or aortas of *Phactr1*^{ECKO}*Apoe*$^{-/-}$ and *Phactr1*$^{f/f}$*Apoe*$^{-/-}$ littermates (n=4), respectively. **B**, Identification of EC-enriched mRNA samples from wild-type mice. Real-time PCR analysis of *Cdh5* and *Acta2* in EC-enriched intima component and remaining media and adventitia tissues (n=4). **C**, *Phactr1* transcript expressions in aortic ECs of *Apoe*$^{-/-}$ mice (n=5) were analyzed by RNA-seq. **D** through **F**, Differentially expressed genes (DEGs) between *Phactr1*$^{-/-}$ and *Phactr1*$^{+/+}$ mice (**D**), and KEGG (**E**) and GO analysis (**F**) of DEGs. **G** through **I**, DEGs between *Phactr1*^{ECKO}*Apoe*$^{-/-}$ and *Phactr1*$^{f/f}$*Apoe*$^{-/-}$ mice (**G**) and KEGG (**H**) and GO analysis (**I**) of DEGs. Data were presented as mean±SEM and analyzed using unpaired two-tailed Student's *t*-test with Welch's correction in **B**, and Kruskal-Wallis test with Dunn's multiple comparisons test in **C**.

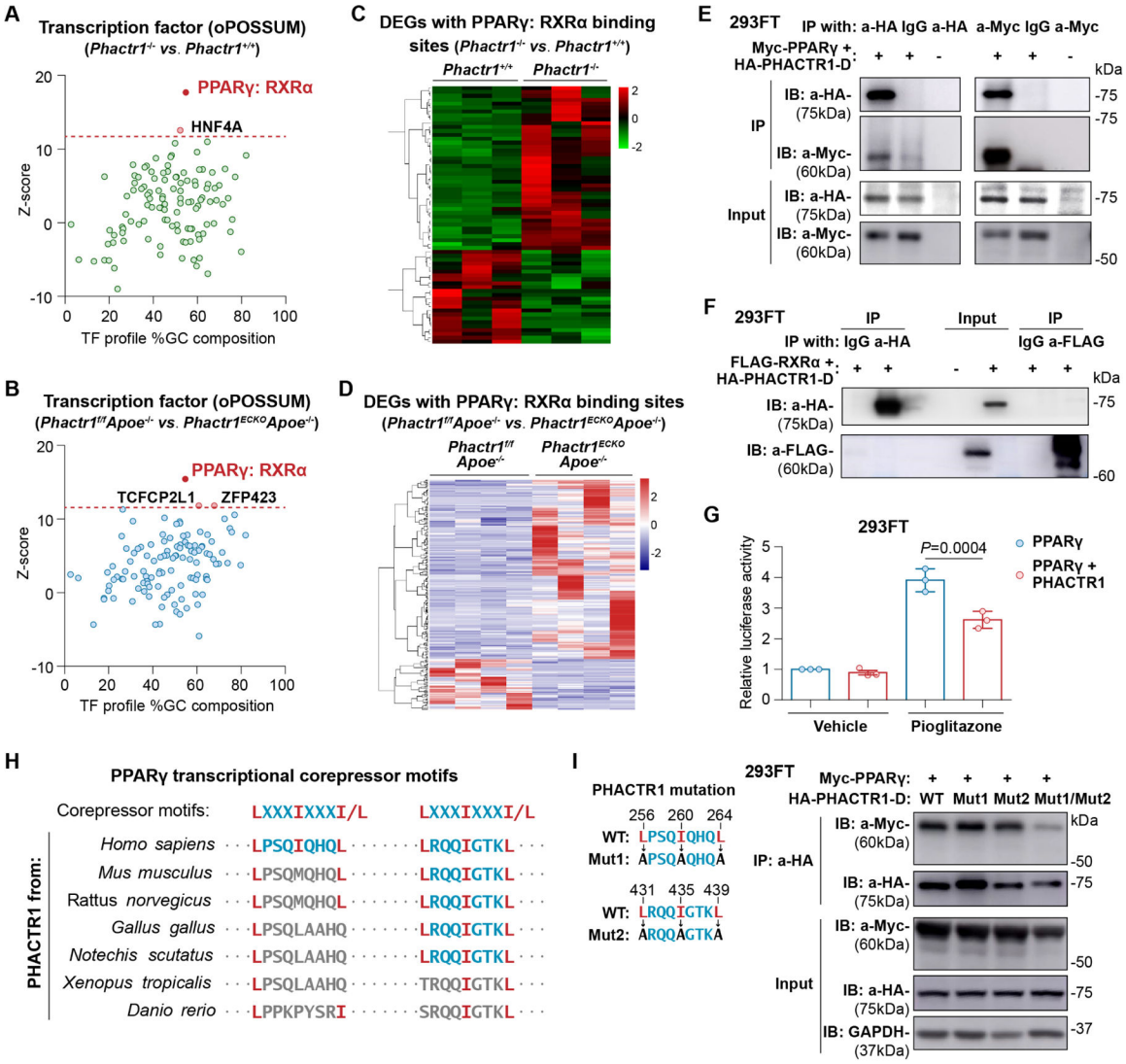

Figure 5. PHACTR1 interacted with PPARγ and repressed PPARγ transcriptional activity.

A and **B**, Transcription factor analysis by oPOSSUM using differentially expressed genes (DEGs) between *Phactr1*$^{-/-}$ and *Phactr1*$^{+/+}$ mice (**A**) or between *Phactr1*^{ECKO}*Apoe*$^{-/-}$ and *Phactr1*$^{f/f}$*Apoe*$^{-/-}$ mice (**B**). **C** and **D**, Expression of DEGs with PPARγ/RXRα binding sites between *Phactr1*$^{-/-}$ and *Phactr1*$^{+/+}$ mice (**C**) or between *Phactr1*^{ECKO}*Apoe*$^{-/-}$ and *Phactr1*$^{f/f}$*Apoe*$^{-/-}$ mice (**D**). **E**, Co-immunoprecipitation in 293FT cells overexpressing Myc-tagged PPARγ and HA-tagged PHACTR1 isoform D. **F**, Co-immunoprecipitation in 293FT cells overexpressing FLAG-tagged RXRα and HA-tagged PHACTR1 isoform D. **G**, PPARγ luciferase activity in PPARγ-overexpressed 293FT cells transfected with PHACTR1 isoform D plasmid or vector control. Luciferase activity was detected after incubating with 10 μM pioglitazone or vehicle control for 12 hours. *n*=3. Data were presented as mean±SEM and analyzed using 2-way ANOVA with Bonferroni's *post hoc* test. **H**, PPARγ corepressor motifs (LXXXIXXXI/L) in PHACTR1 proteins from different species. **I**, Co-immunoprecipitation in 293FT overexpressing Myc-tagged PPARγ and wild-type (WT) or PPARγ corepressor motif-mutated PHACTR1 isoform D (HA-tagged). Mut1: L256A/

I260A/L264A mutation in PHACTR1 isoform D, Mut2: L431A/I435A/L439A mutation in PHACTR1 isoform D.

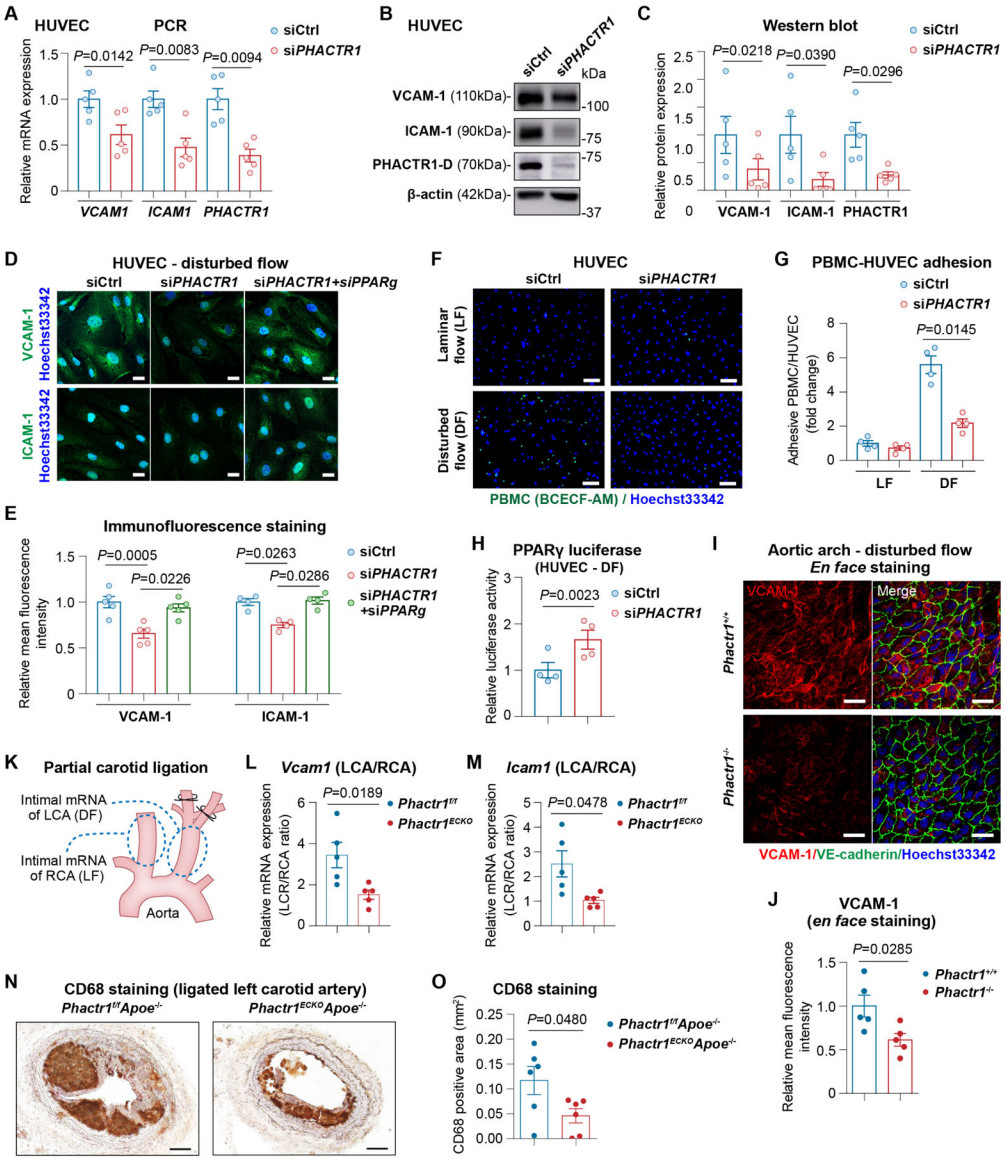

Figure 6. PHACTR1 was required for endothelial cell activation in response to disturbed flow.

A, *VCAM1*, *ICAM1* and *PHACTR1* mRNA expression was determined by real-time PCR in HUVECs after *PHACTR1* knockdown by siRNA (si*PHACTR1*) for 48 hours. n=5. **B** and **C**, Immunoblot analysis and quantification of VCAM-1, ICAM-1 and PHACTR1 isoform D (PHACTR1-D) in HUVECs after *PHACTR1* knockdown by siRNA (si*PHACTR1*) for 48 hours. n=5. **D** and **E**, Immunofluorescence staining and quantification of VCAM-1 and ICAM-1 in HUVECs treated with negative control siRNA (siCtrl) or si*PHACTR1* plus si*PPARg* for 48 hours followed by disturbed flow (DF) for 16 hours. Scale bars: 20 μm. n=5. **F** and **G**, PBMC adhesion to HUVECs after *PHACTR1* knockdown by siRNA (si*PHACTR1*) for 48 hours followed by DF or laminar flow (LF) for 24 hours. Scale bar: 100 μm. n=4. **H**, PPARγ luciferase activity was detected in HUVECs after *PHACTR1* knockdown and treatment with DF for 12h. n=4. **I** and **J**, *En face* staining and quantification of VCAM-1 in disturbed flow regions of aortic arch from *Phactr1*$^{+/+}$ and

Phactr1$^{-/-}$ littermate control mice (n=5). Scale bars: 20 μm. **K** through **M**, Endothelial *Vcam1* and *Icam1* mRNA expression in partially ligated carotid arteries from *Phactr1*^{ECKO} and *Phactr1*$^{f/f}$ littermates (n=5). Partial ligation was performed and intimal RNA was collected from left carotid artery (LCA) and right carotid artery (RCA) 3 days after surgery. *Vcam1* and *Icam1* was determined by real-time PCR and shown as the ratio of mRNA expression of ligated LCA to sham-operated RCA. **N** and **O**, Macrophages in atherosclerotic lesions were stained by CD68 and quantified in frozen section of ligated carotid arteries at post-surgery day 14 (n=6). Scale bars: 50 μm. Data were presented as mean±SEM and analyzed using paired two-tailed Student's t-test in **A**, **C, G** and **H**, repeated measures one-way ANOVA with the Greenhouse-Geisser correction followed by Dunnet's *post hoc* test in **E**, and unpaired two-tailed Student's t-test without correction in **J**, **L** and **O** and with Welch's correction in **M**. Cell experiments used HUVECs of passages 3 to 5 from at least three donors.

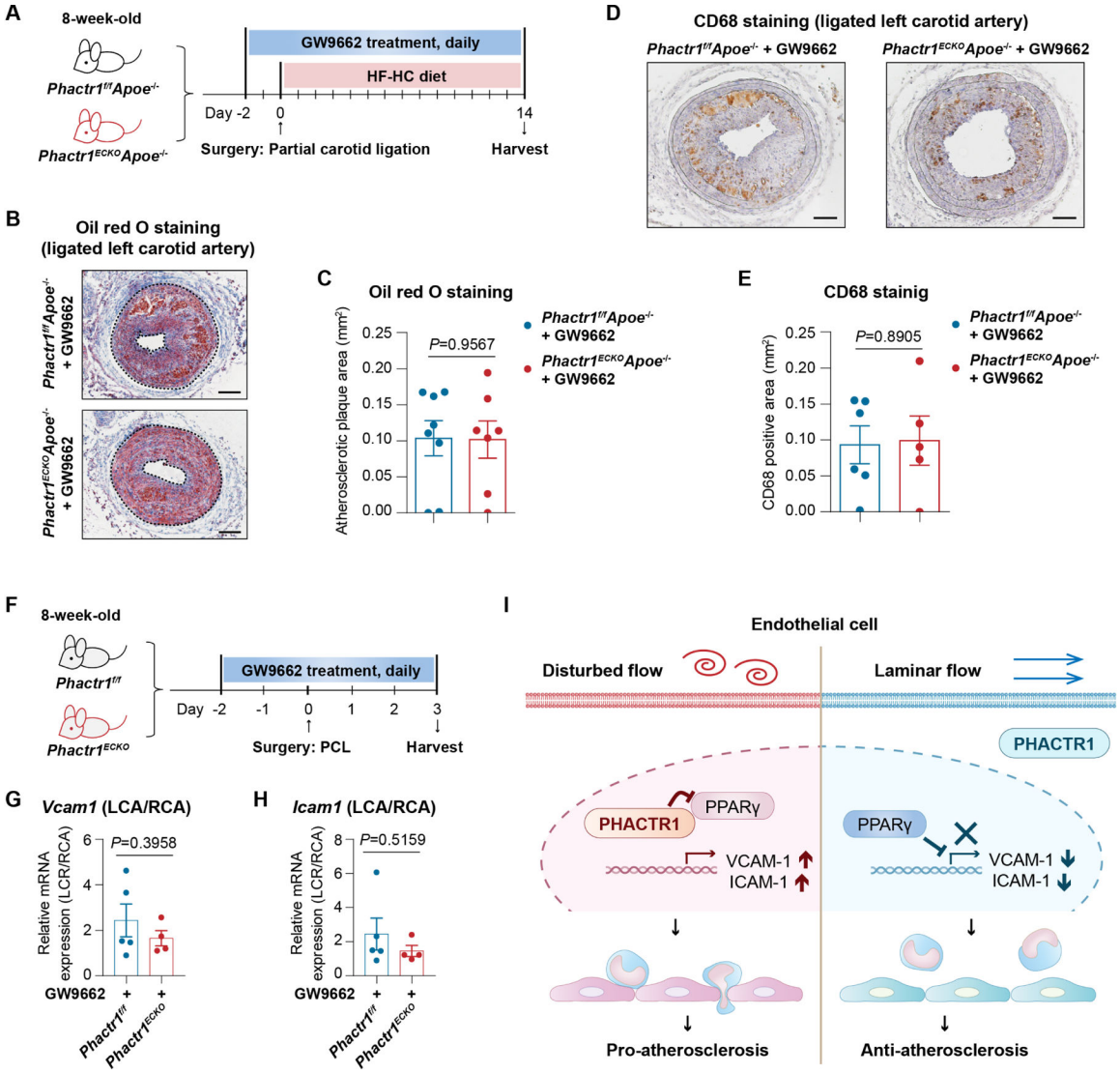

Figure 7. PPARγ antagonist GW9662 eliminated the protective effects of *Phactr1* depletion on endothelial activation and atherosclerosis *in vivo*.

A through **C**, Partial carotid ligation was performed in *Phactr1*^{ECKO}*Apoe*$^{-/-}$ (n=7) and *Phactr1*$^{f/f}$*Apoe*$^{-/-}$ mice (littermates, n=8) with pre-surgery GW9662 treatment (qd, 3.6 μmol/kg body weight (1mg/kg body weight), i.p.) for 2 days. Then mice were given the HF-HC diet and GW9662 treatment for two weeks. Atherosclerotic lesions were analyzed by oil red O staining and quantified in frozen section of ligated carotid arteries at post-surgery day 14. Scale bars: 100 μm. **D** and **E**, Macrophages in atherosclerotic lesions were stained by CD68 and quantified in frozen section of ligated carotid arteries of *Phactr1*^{ECKO}*Apoe*$^{-/-}$ (n=6) and *Phactr1*$^{f/f}$*Apoe*$^{-/-}$ mice (littermates, n=5) at post-surgery day 14. Scale bars: 50 μm. **F** through **H**, Partial carotid ligation was performed in *Phactr1*^{ECKO} (n=4) and *Phactr1*$^{f/f}$ mice (littermates, n=5), and GW9662 (3.6 μmol/kg body weight (1mg/kg body weight), i.p.) was administrated once daily from pre-surgery day 2 to post-surgery day 2. Left carotid arteries (LCAs) and right carotid arteries (RCAs) were harvested and intimal mRNA was extracted post-surgery day 3. *Vcam1* and *Icam1* expression was determined

by real-time PCR and shown as the ratio of mRNA expression of ligated LCA to sham-operated RCA. **I**, Proposed model for endothelial PHACTR1 in endothelial activation and atherosclerosis. Under laminar flow, PHACTR1 existed in the cytoplasm and PPARγ inhibited inflammation. In regions of disturbed flow, PHACTR1 was located in the nucleus, interacted with PPARγ as its transcriptional corepressor and upregulating expression of adhesion molecules on cell surface. Leukocytes attached to endothelial cells and infiltrated into the vessel wall to promote atherosclerosis. Data were presented as mean±SEM and analyzed using unpaired two-tailed Student's *t*-test without correction in **C**, **E** and **G**, and with Welch's correction in **H**.